NOA-D-19-00065R2

Constitutive activation of the EGFR-STAT1 axis increases proliferation of meningioma tumor cells

Sara Ferluga[1], Daniele Baiz[1], David A. Hilton[2], Claire L. Adams[1], Emanuela Ercolano[1], Jemma Dunn[1], Kayleigh Bassiri[1], Kathreena M. Kurian[3] and C. Oliver Hanemann[1, 4]

[1] University of Plymouth, Faculty of Health: Medicine, Dentistry and Human Sciences, The Institute of Translational and Stratified Medicine, The John Bull Building, Plymouth Science Park, Research Way, Plymouth UK, PL6 8BU

[2] Cellular and Anatomical Pathology, Plymouth Hospitals NH Trust, Derriford Road, Plymouth UK, PL6 8DH

[3] Department of Neuropathology, Pathology Sciences, Southmead Hospital, Southmead Road, Bristol UK, BS10 5NB

[4] **Corresponding author**: Prof. Clemens Oliver Hanemann MD, FRCP, Director of the Institute of Translational and Stratified Medicine, University of Plymouth, Faculty of Health: Medicine, Dentistry and Human Sciences, Plymouth Science Park, Research Way, Plymouth UK, PL6 8BU. Phone: +44 1752437418, Fax: +441752517846, E-mail: Oliver.Hanemann@plymouth.ac.uk

Running Title: EGFR-STAT1 tumor-promoting role in meningioma

Funding: This work was funded by Brain Tumour Research. DB was partially funded by the FP7 Marie Curie Actions (PCOFUND-GA-20126001). Tissue samples were obtained from University Hospitals Plymouth as part of the UK Brain Archive Information Network (BRAIN UK) which is funded by the Medical Research Council.

Conflict of Interest: Authors declare that there are no conflicts of interest.

Authorship: Designing and execution of most of the experiments, data interpretation, manuscript and figures preparation – SF

Designing and execution of gene expression studies, data interpretation, writing of the related part, performing experimental revisions and addressing comments to reviewers, proofreading of the manuscript – DB

Designing and execution of immunohistochemistry, data interpretation, writing of the related part – DAH

Designing and execution of the flow cytometry experiments, data interpretation, writing of the related part – CLA

Managing of tumor digestions and primary MN cells cultures – EE

Supporting with Western blot studies on MN Merlin status – JD

Supporting with the initial identification of STAT1 in meningioma – KB

Providing the majority of the samples involved in the study – KMK

Intellectual input to the critical design of the study, data interpretation, ~~proofreading of the~~ manuscript preparation - COH

Total Word Count: ~~6065~~6217

Abstract

Background: Meningiomas are the most frequent primary brain tumors of the central nervous system. The standard of treatment is surgery and radiotherapy, but effective pharmacological options are not available yet. The well-characterised genetic background stratifies these tumors in several subgroups, thus increasing diversification. We identified EGFR-STAT1 overexpression and activation as a common identifier of these tumors.

Methods: We analysed STAT1 overexpression and phosphorylation in 131 meningiomas of different grades and locations by utilising several techniques, including Western blots, qPCR and immunocytochemistry. We also silenced and overexpressed wild-type and mutant forms of the gene to assess its biological function and its network. Results were further validated by drug testing.

Results: STAT1 was found widely overexpressed in meningioma but not in the corresponding healthy controls. The protein showed a constitutive phosphorylation not dependent on the JAK/STAT pathway. *STAT1* knock-down resulted in a significant reduction of cellular proliferation and deactivation of AKT and ERK1/2. STAT1 is known to be activated by EGFR, so we investigated the tyrosine kinase and found that EGFR was also constitutively phosphorylated in meningioma and was responsible for the aberrant phosphorylation of STAT1. The pharmaceutical inhibition of EGFR caused a significant reduction in cellular proliferation and of overall levels of Cyclin D1, pAKT and pERK1/2.

Conclusions: STAT1 EGFR-dependent constitutive phosphorylation is responsible for a positive feedback loop that causes its own overexpression and consequently an increased proliferation of the tumor cells. These findings provide the rationale for further studies aiming to identify effective therapeutic options in meningioma.

Keywords: Meningioma, STAT1, EGFR, cancer, brain

Importance of the Study

Meningioma accounts for 37% of primary brain tumors. This year in the United States an estimated thirty-two thousand people will be diagnosed with meningioma. ~~Despite the majority of t~~These tumors ~~are benign in nature, they~~ can cause mild to severe morbidity and even WHO grade I ~~eventually progress to~~can have a more aggressive ~~phenotype~~clinical course. Therapeutic options are still limited to surgical resection and radiotherapy since more effort is needed to decipher the communal molecular mechanisms that define meningiomas despite their genetic background.

Aiming to discover novel therapeutic targets, we identified STAT1 as aberrantly overexpressed and constitutively activated in most of the meningioma examined. Its activation is dependent on the constitutive phosphorylation of EGFR and leads to an increased proliferation of tumor cells. We show that specific EGFR inhibition can reduce tumor cell proliferation and we show evidence why previous trials failed. Therfore, we suggest that this therapeutic strategy be re-evaluated.

Introduction

Meningiomas are the most common primary brain tumors, classified meningiomas as Grade I (~80%), atypical Grade II (15-20%) and anaplastic/malignant Grade III (1-3%). Surgery is the primary choice of treatment; complete resection may be curative but it can be achieved only for permissive locations[1]. The genetic background of meningioma is well characterised, with inactivation/deletion of *NF2* found in ~60% of sporadic meningiomas[2].

Previously, we identified phosphorylated Signal Transducer and Activator of Transcription 1 (STAT1) as overexpressed in the grade I meningioma cell line [3] and phosphorylated STAT1 in meningioma tissue of all grades[4]. In addition, we identified phosphorylation of STAT3 among remaining STAT family members[3,4]. STAT1 belongs to the STAT protein family that comprise seven members (STAT1-4, STAT5A, STAT5B and STAT6), and it can be phosphorylated on the tyrosine 701 (Y701) and the serine 727 (S727)[5,6]. STATs are essential components of the evolutionarily conserved JAK/STAT signalling pathway[4,7] that plays a role in immune response[8,9] and its dysregulation is linked to cancer[10,11]. This canonical pathway is activated by ligands including interferons, interleukins and some growth factors, binding to their receptors thus inducing phosphorylation of the JAKs (Janus Kinases), leading to ~~to~~ tyrosine-STAT phosphorylation by JAKs[4,6]. In addition STATs can also~~s~~ be phosphorylated by receptor tyrosine kinases and cytoplasmic non-receptor tyrosine kinases[5]. Phosphorylated STATs homo- and hetero-dimerize entering the nucleus to regulate transcription of target genes[6,12]. JAKs include JAK1-3 and TYK2. JAK1 and JAK2 are phosphorylated following type-II interferon (IFNγ) stimulation, while JAK1 and TYK2 are activated in type-I interferon signalling (IFNα, IFNβ; etc.)[4-6]. Activated JAK/STAT pathway can be quenched by the SOCSs (Suppressors Of Cytokine Signalling), the PIASs (Protein Inhibitors of Activated STAT) and the PTPs (Protein Tyrosine Phosphatases)[5]

Activated STAT1 acts as a transcriptional regulator, controlling its own transcription as well as the expression of several IFN-regulated genes (IRGs)[13,14]. STAT1 was considered a tumor suppressor as its expression correlated with good prognosis in several types of cancer[15-18]. However, other studies established a pro-tumorigenic role of STAT1, which correlated with its overexpression and activation[19]. Due to its function in sensing and regulating cytokine production, STAT1 exerts a role in promoting an immunosuppressive tumor environment[19,20]. Hence, the overall role of STAT1 in cancer remains complex suggesting that its function is most likely cancer type-dependent.

Formatted: Indent: First line: 0"

In the present study, we identified STAT1 as overexpressed and phosphorylated in meningioma compared to normal and we show that its overexpression correlates with an increased proliferation of the tumor cells as well as an activation of AKT and ERK1/2. We demonstrate that STAT1 overexpression and phosphorylation is not dependent on the JAK/STAT pathway but it depends on a positive feedback loop caused by the constitutive activation of the Epidermal Growth Factor Receptor (EGFR). The pharmaceutical inhibition of EGFR in meningioma caused the deactivation of STAT1 and other cancer-related pathways, eventually leading to a significant reduction in cellullar proliferation. Our findings underline a crucial role of the EGFR and STAT1 signalling in the pathology of meningiomas and point to a therapeutic potential of its inhibition.

Materials and Methods

Meningioma specimens, tumor digestion and primary meningioma cultures

Meningioma specimens were collected following the ethical approvals ~~(REC: 14/SW/0119; IRAS project ID: 153351; Plymouth Hospitals NHS Trust: R&D: 14/P/056, North Bristol NHS Trust: R&D: 3458)~~ received a unique MN number~~. J specimens were collected via UK Brain Archive Information Network (BRAIN UK; Ref.:15/011; REC: 14/SC/0098)~~ (Supplementary Table 1). Normal meningeal tissue (NMT) was purchased from Analytical Biological Service Inc.

Primary cells were generated from 36 fresh t~~T~~umor tissues~~.~~ Tissue were disaggregated in DMEM with 15% FBS, 100 U/ml penicillin/streptomycin and 20 U/ml Collagenase III (Worthington Biochemical Corp) for 2 h at 37 °C; after cells were pelleted at 1000 rpm for 5 min, resuspended and seeded (modified from[21]). MN cells were cultured in DMEM at 37 °C in 5% CO2. HMC cells (Caltag Medsystems Ltd) were grown in the recommended medium at 37 °C in 5% CO_2. Cells were kept on average 4-5 passages.

Normal human meningeal cell were purchased from ScienceCell (UK distributor: Caltag Medsystems; Catalog#1400), U251 glioma cells were purchased from ECACC (Cat n.: 09063001), an immortalized grade 1 meningioma cell line BM-1 were (DSMZ; Cat.n.: ACC 599) and authenticated via genomic fingerprinting (Eurofins Genomics Europe Applied Genomics GmbH).

Formatted: Font: 10 pt
Formatted: Normal, Left
Formatted: Font: 10 pt
Formatted: Font: 10 pt
Formatted: Font: 10 pt

Western blotting, immunofluorescence and immunohistochemistry

Western blots (WB) from 26 frozen tissues and cell cultures were performed as previously described[3]. All primary antibodies used are listed in Supplementary Table ~~1~~2. Immunoreactive bands were quantified using Scion Image software and each band was normalized *vs.* the corresponding GAPDH.

Immunofluorescence of 38 paraffin embedded tissue was performed as previously described[3]. Confocal microscopy was executed using a Leica DMI6000B; Z-stack micrographs were taken using the 40X or 63X objectives. Immunofluorescent images for STAT1-silencing studies were taken with the Olympus CKX41 with the 20X objective; images were processed with the QCapture Pro 6.0 software.

For immunohistochemistry, paraffin sections (4μm) were processed as described[22]. Avidin-biotin blocking solution was used with EDTA pretreatment. Sections were incubated with appropriate biotin-labelled secondary antibody and with horseradish peroxidase for detection using Vectashield Elite (Vector Laboratories UK) according to the manufacturer's protocol. As a control, sections were incubated with omission of the primary antibody.

Results were reviewed 'blind' to the histological grade by a neuropathologist (DAH). Semiquantitaive assessment of the intensity of immunoreactivity was undertaken and scored as follow: 0 none; 1 weak; 2 moderate; 3 strong.

RNA isolation and gene expression analysis

Total RNA was extracted from 95 frozen tissues and cells using the Qiazol® reagent (Qiagen UK), following manufacturer's protocol. The quality, integrity and concentration of RNA were established using the NanoDrop ND-2000 (ThermoFisher Scientific UK).

Real-Time PCR (qPCR) was conducted using 50 ng/well employing the EXPRESS One-Step SYBR® GreenERTM kit (Invitrogen) on a LightCycler® 480 System (Roche Diagnostics, Switzerland), following manufacturer's protocol (primers annealing temperature= 58 °C). Primers used were: PrimePCR™ SYBR® Green Assay STAT1 (BioRad), hGAPDH (2 μM, Invitrogen- Forward: 5'-GAGAAGGCTGGGGCTCATTT-3'; Reverse 5'-AGTGATGGCATGGACTGTGG-3'). Relative gene expression analysis of STAT1 and GAPDH was calculated using the $2^{-\Delta\Delta Ct}$ method[23], employing the HMC as calibrator.

STAT1 silencing and overexpression

Stat1 shRNA Lentiviral Particles (Santa Cruz Biotechnology, sc-44123-V), containing 3 target-specific constructs that encode 19-25nt (plus hairpin) or scramble shRNA control (Santa Cruz Biotechnology, sc-108080), were added onto the cells in media containing protamine sulfate salt (8 μg/ ml) (Sigma). Cells were infected for 48 h before applying puromycin (5 μg/ml) for 3 days.

STAT1-WT gene was cloned into pCDNA3.1+ in a two-step process using the following primers: STAT1-F1 (5'-AAAGCTAGCGGCCGGCCATGTCTCAG-3'), STAT1-R1 (5'-CGTCTCGAGGTCAATTACCAAACCAGGCT-3') for the first part; STAT1-2F (5'-GACCTCGAGACGACCTCTCT), STAT1-2R (5'-AGTGTTTAAACTTAATTAACTATACTGTGTTCA-3')

Formatted: Indent: First line: 0"

for the second part. The 551 bp long STAT1 part in between the restriction sites HindIII and EcoRI was synthesised (GeneArt, ThermoFisher Scientific) to generate the following mutations: Y701F, S727E and Y701F/S727E; each one was cloned into pCDNA-STAT1-WT to replace the wild-type part. All generated plasmids were sequenced before further use (Eurofins). U251-MG cells were transfected and selected as previously described [24].

Ki-67 staining and Proliferation assay

For Ki-67 staining, cells were grown on chamber slides, lentivirus-transfected and stained as previously described[3].

For U251-MG proliferation assay, the pool of U251-MG selected cells, transfected with pCDNA, STAT1-WT and the three mutants, were seeded at 1000 cell/well in 96 well plates and proliferation was determined after 24, 48 and 72 h using the 'CellTiter-Glo® Luminescent Cell Viability Assay' as recommended by the supplier (Promega).

For drug testing, meningioma cells (~3000 cell/well) were plated in 96-well culture plates and allowed to proliferate for 24 h. Cell proliferation was calculated as percentage of control cells. Graphs were generated using GraphPad Prism 5.

Flow cytometry analysis

Confluent meningioma cells were resuspended in ice-cold staining buffer (PBS, 2%FBS) at a final concentration of $1x10^5$ cells. Cells were stained for 30 min at RT in the dark with the following: CD45-FITC, HLA-DR-PE, CD14-PerCP5.5 and CD44 –APC (Becton Dickinson Biosciences, Pharmigen), washed twice with 2 ml of staining buffer and centrifuged at 1500 rpm for 5 min at 4°C . The relevant single isotype controls were used. Data acquisition was collected on $1x10^4$ cells on a Accuri flow cytometer (BD Biosciences) and analysis was performed using the Flow Jo software v10.0 (FlowJo LLC, Ashland, OR).

Statistical analysis

Probability (p) values were calculated using the Student's t-Test or the ANOVA one-way analysis of variance, using GraphPad Prism 5.01 and MS Excel 2016 software. P values <0.05 were considered statistically significant. The results are expressed as means ± SD or ± SEM.

Formatted: Indent: First line: 0"

Results

STAT1 is overexpressed and aberrantly activated in meningioma

We analysed STAT1 expression in meningioma tumors compared to normal meninges (NMT). In all cases STAT1 was overexpressed and in most of the cases, we detected high levels of phosphorylated STAT1 (Y701 and S727) (representative Western blot of Fig. 1A and qPCR of Fig. 1C). Immunohistochemical studies validated STAT1 overexpression in all meningioma samples (Fig. 1B); also pSTAT1-Y701 and -S727 showed higher staining compared to normal meninges and an increasing score throughout the grades. As control, we further analysed STAT1 and pSTAT1 abundance in two additional normal meninges and a normal brain (Fig. 1D).

Then, we examined STAT1 expression and phosphorylation in meningioma-derived primary cells (MN) and in BM-1[25] compared to HMC. MN cells were used between passage 3 and 5 and no B/T lymphocytes or infiltrating macrophages were detected (Supplementary Fig. 1A). All cells were vimentin-positive[26] and CD90-negative, suggesting no fibroblasts contamination[27] (Supplementary Fig. 1B). STAT1 was found overexpressed in BM-1 and MNs compared to HMC and both pSTAT1-Y701 and -S727 were present across all samples while faint and undetectable in HMC (Fig. 1C). Q-PCR analysis confirmed that *STAT1* expression was higher in most of the MNs and in BM-1 compared to control (Fig. 1F). Of note, STAT1 overexpression was independent of Merlin status (Supplementary Fig. 1C, D).

Furthermore, pSTAT1-Y701 showed a cytoplasmic localization while pSTAT1-S727 was nuclear (Fig. 1B), in agreement with the immunofluorescent staining of primary MN cells (Fig. 1G).

Overall, we examined 131 meningiomas *vs.* 10 normal meninges and 5 normal brains and we demonstrate substantial overexpression of STAT1 in 100 of them with a variety of methods (Supplementary Table 12).

STAT1 constitutive phosphorylation is not dependent on the JAK/STAT pathway

To further investigate STAT1 phosphorylation in the context of the tumor environment, we examined meningioma tumor lysates for the presence of interferon gamma (IFNγ) and tumor-associated

Formatted: Indent: First line: 0"

macrophages by using CD163 marker staining preferentially M2 macrophages [28]. Variable protein levels of IFNγ and CD163 were detected, but there was no evident correlation with STAT1 phosphorylation and no JAK1 phosphorylation was detected (Fig 2A).

STAT1 usually becomes phosphorylated as a result of JAK/STAT pathway activation in response to external stimuli[6]. We examined whether STAT1 overexpression and phosphorylation was dependent on the culture conditions and secreted factors. Culturing HMC in serum-free (SF) media and in BM-1 conditioned media, and BM-1 in SF media, we confirmed that STAT1 overexpression and phosphorylation was not due to external factors, but most likely to an intrinsic activation (Fig. 2B).

Next, we decided to test the ability of the JAK/STAT pathway to respond to activating stimuli in meningioma cells. HMC and two MNs were treated with IFNγ; in HMC, JAK1 and JAK2 activated within 10 min after treatment as well as pSTAT1-Y701 whilst pSTAT1-S727 phosphorylated within 1 h. The same behaviour was observed in MNs confirming that the JAK/STAT pathway was functional; however, STAT1 was constitutively phosphorylated in non-treated cells while pJAK1 and pJAK2 were not (Fig. 2C). The same experiment, performed using interferon alpha (IFNα), produced comparable results (Supplementary Fig. 2A).

Formatted: Indent: First line: 0"

After activation, pSTAT1 is known to dimerize and translocate into the nucleus[6]. IFNγ treatment was indeed able to induce pSTAT1-Y701 nuclear internalization (Fig. 2D, Supplementary Fig. 2B). Thus, the JAK/STAT1 pathway can be activated *via* IFN in meningioma cells but there was also an IFN-independent intrinsic activation.

STAT1 constitutive phosphorylations could be due to a deficient deactivation of the pathway[4,5,29]. Thus, we analysed the levels of the SOCSs and the PIASs in HMC, BM-1 and MN cells (Fig. 2E), which did not correlate with the constitutive phosphorylation of STAT1 observed in these samples (Fig. 1E).

Overall, these data suggest that the JAK/STAT pathway is functional but not over-activated. Therefore, we hypothesized other mechanisms must be involved in maintaining STAT1 in a constitutive phosphorylated form in the meningioma samples analyzed.

STAT1 overexpression is associated with an increased proliferation of meningioma cells

To investigate the biological significance of STAT1 overexpression in meningioma we silenced the protein in MN cells. Lentiviral-mediated shRNA delivery into the cells produced an over 70% reduction in protein expression (Fig. 3A) and a 50% reduction in gene expression levels compared to scramble

(Fig. 3B). STAT1-silenced cells displayed a reduction in STAT1 immunofluorescent staining as well as a reduction in Ki67-positive cells (Fig. 3C). Proliferating cells were reduced from ~22% to less than 5% in MNs (Fig. 3D, E). This was in agreement with the reduction of the total number of cells (Fig. 3F) and a 40% reduction of Cyclin D1 (Fig. 3A). A similar effect was observed in BM-1 cells (Supplementary Fig. 3A-D). Taken together, our results demonstrate that STAT1 overexpression is associated to an increased proliferation of meningioma tumor cells.

The MAPK-ERK and the AKT pathways are known to be active in meningioma and to influence tumor progression[30]. After STAT1-KD, both AKT and ERK1/2 showed a 95% and 80% reduction in protein phosphorylation respectively (Fig. 3G, H), supporting a critical involvement of STAT1 in the activation of pro-proliferative pathways.

Phosphorylated STAT1 affects activation of AKT and ERK1/2 and cellular proliferation

We used phosphomimetics to further characterise the effects of STAT1 phosphorylation. Phenylalanine (F) and Glutamic acid (E) are used to mimic the structure of a phosphorylated tyrosine (Y) and phosphorylated serine (S) respectively[31]. We produced three different STAT1 mutants: Y701F, S727E and the double mutant Y701F/S727E. Since STAT1 is constitutively phosphorylated in meningioma, we used U251-MG cells as a model because this cell line showed levels of total and pSTAT1 lower than HMC (Fig. 4A). STAT1 overexpression in U251-MG for wild-type (WT) and mutants was confirmed by WB and qPCR (Fig. 4B, C). STAT1 overexpression in U251-MG cells determined an increased phosphorylation of AKT and ERK1/2, where the effect was particularly evident for pERK1/2 in STAT1-S727E and STAT1-Y701F/S727E mutants (Fig. 4B).

The proliferation of transfected cells was measured over a period of 72 h and normalised for the empty-vector control. All STAT1 mutants showed a significantly increased proliferation rate compared to STAT1-WT; interestingly, the double mutant STAT1- Y701F/S727E, which represents STAT1 in its maximal activated condition, determined the highest pro-proliferative effect in U251-MG cells (Fig. 4B, 4D).

These experiments confirmed that the constitutive phosphorylation of STAT1 on both phosphosites affects the activation of the AKT and ERK1/2 pathways as well as the proliferation of the cells in agreement with STAT1 knock-down results in meningioma.

EGFR constitutive phosphorylation is responsible for STAT1 overexpression and activation

Formatted: Indent: First line: 0"

Formatted: Indent: First line: 0"

It has been previously shown that STAT1 can be phosphorylated by EGFR, a key tyrosine kinase relevant to the majority of tumors[32,33]. We examined the EGFR status in meningioma tissues and cells, detecting high levels of pEGFR in both tumor lysates and meningioma cells, when compared to normal meningeal tissue (NMT) and HMC (Fig. 5A).

To test whether the constitutive phosphorylation of EGFR was responsible for STAT1 phosphorylation, we treated BM-1 cells with three different EGFR inhibitors (canertinib andafatinib, 2nd generation irreversible inhibitors) and erlotinib (1st generation, reversible inhibitor), , for 30 min, 3, 6 and 24 h[34]. Canertinib (and similarly afatinib) decreased STAT1 expression of about 60% within 24 h upon; pSTAT1-Y701 was almost abolished 30 min after treatment but was restored at 24 h while pSTAT1-S727 showed a decrease of about 90% compared to vehicle at 24 h (Fig. 5B). Almost no effect on total and pSTAT1 was detected after treatment with erlotinib, which did not cause an evident decrease in pEGFR-Y1068 after treatment (Fig. 5B).

EGFR blockade *via* canertinib and afatinib decreased pSTAT1 levels and determined a concentration-dependent decrease of cellular proliferation already at 24 h after treatment (Fig. 5C), with erlotinib being ineffective.

Since canertinib showed the strongest effect on STAT1 in BM-1 cells, we tested its effects on primary MNs (Fig. 5D). Canertinib was active in reducing EGFR constitutive phosphorylation in MN cells, reducing p-STAT1 levels after canertinib treatment; pSTAT1-S727 reduced of 65% already 3 h after treatment and stayed low over the 24 h; phosphorylated STAT1-Y701 also showed about 50% reduction 3 h after treatment and recovered between 6 and 24 h (Fig. 5D, E Supplementary Fig. 4).

Phospho-AKT and pERK1/2 showed a decrease of about 70% and Cyclin D1 reduced t0 50% in 24 h (Fig. 5D,E,Supplementary Fig. 4).

We wanted to examine whether the inhibition of pEGFR and thus of pSTAT1 had any effect on *STAT1* expression, as STAT1 is known to regulate its own transcription[35]. *STAT1* expression levels reduced by ~50% 24 h after treatment with canertinib in MNs (Fig. 5F), consistently with a 30% reduction in protein level observed by WB analysis (Fig. 5D, E, Supplementary Fig. 4).

Lastly, to confirm the link between EGFR activation and STAT1 phosphorylation, we treated BM-1 cells with the Epidermal Growth Factor (EGF) for 5, 30 and 60 minutes. Upon EGF treatment STAT1 was phosphorylated on Y701 within 5 minutes and on S727 within 30 minutes (Fig. 5G).

Hence, we showed that EGFR is responsible for STAT1 overexpression and constitutive activation in meningioma, which consequently increases proliferation of the tumor cells.

Formatted: Indent: First line: 0"

Discussion

Meningiomas are the most common primary brain tumor but there are no therapeutic options available other than surgery and radiotherapy[1,36]. The well-defined genetic background of meningioma is leading towards an increasing stratification of these tumors into subtypes[37,38]; however, common features should still be investigated.

We identified STAT1 as overexpressed and activated in 84% of meningioma examined. The only study exploring the expression levels of STAT and JAK superfamilies in meningiomas was published in 1999 showing higher immunoreactivity of JAK1 (see also Supplementary Fig. 2C), JAK2 and the STATs in meningiomas compared to normal dura[39]. Our data confirmed the expression of the JAKs in MN cells and in HMC; we showed that the JAK/STAT pathway is activated by IFNα and IFNγ, inducing nuclear localization of pSTAT1 as seen before[39]. As previously reported[40], activation of STAT1 after INFγ stimulation occurs via JAK kinases by phosphorylation on Y701, resulting in pSTAT1 translocation into the nucleus and subsequent phosphorylation at S727[41]. Double phosphorylation is required for maximal STAT1 activity. However, we show that STAT1 is constitutively phosphorylated in MNs but not in HMC, even without IFN stimulation and in serum-free conditions. In tumor lysates, STAT1 phosphorylation was not consistent with the presence of M2-polarised macrophages or IFNγ suggesting that the constitutive activation of STAT1 was not related to the JAK/STAT pathway.

To better understand the meaning of this STAT1 phosphorylation we used phosphomimetics, generating STAT1-Y701F, STAT1-S727E and STAT1-Y701F/S727E mutants. The overexpression of these mutants induced activation of two central nodes in cancer signalling, AKT and ERK1/2, and

Formatted: Left, Indent: First line: 0", Don't adjust space between Latin and Asian text, Don't adjust space between Asian text and numbers

Formatted: Indent: First line: 0"

increased cellular proliferation. A similar approach was used on STAT3 in human prostate cancer cell, where the mutant STAT3-Y705F/S727E promoted survival, growth and invasion. They showed that the mutation S727E was increasing the transcription of c-Myc, which is an essential activator of cell growth and proliferation[31]. It is very likely that a similar mechanism is happening also in meningioma, where STAT1-S727 showed a predominant nuclear localization exerting its role of transcriptional regulator.

We also showed the link between STAT1 overexpression and the increased proliferation of the tumor cells. This effect is most likely linked to an activating cascade involving ERK1/2 and AKT, since their activated state and cell proliferation were almost aborted after STAT1 silencing. The activation of the MAPK pathway is involved in both proliferation and apoptosis in meningioma[30], and we recently published a proteomic profiling of meningioma, identifying the aberrant activation of the PI3K/AKT pathway across all meningioma grades[4].

Aiming to identify the kinase responsible for STAT1 activation, we examined the status of EGFR, a tyrosine kinase able to phosphorylate STAT1[33,42,43]. EGFR was overexpressed and constitutively phosphorylated on Y1068 in all of the MN cells examined but not in HMC. To test whether EGFR phosphorylation was responsible for the constitutive activation of STAT1 we used three specific EGFR inhibitors canertinib, afatinib and erlotinib[44]. Whilst canertinib and afatinib, had a similar effect in reducing STAT1 phosphorylation on both phosphosites as well as on cell proliferation and viability, erlotinib, did not produce any significant effect. Interestingly this result is consistent with the unsuccessful clinical trial of erlotinib on recurrent meningiomas[45]. Erlotinib is a first generation ATP dependent reversible rather broad inhibitor[46], Afinitinib and Canertinib are non reversible second generation with high pEC50 https://www.proteomicsdb.org/#analytics/selectivity

In MN cells, canertinib (and afatinib) caused the de-phosphorylation of STAT1-Y701 and S&27 within 6and 24H respectively. Similarly, EGF stimulation induces an immediate and direct phosphorylation on Y701 and a later one on S727, suggesting the activation of an additional kinase downstream of EGFR, which is probably part of the MAPK/ERK1/2 pathway[47]. Indeed previous studies in pancreatic cancer demonstrated the relationship between EGFR and the downstream signalling regulators like pAKT, pERK1/2 and Cyclin D1[33]. In agreement, after canertinib treatment and after STAT1 silencing, we observed a significant reduction of pAKT and pERK1/2. Overall, levels of Cyclin D1 also displayed a significant reduction, consistently with the reduction in proliferation observed after STAT1 silencing and canertinib treatment.

The observed reduction in STAT1 expression suggest a feedback regulatory mechanism of pSTAT1 on its own promoter, already documented[35], as well as an EGFR/HER2-dependent regulation as previously shown in glioblastoma and breast cancer cell lines[48].

In conclusion, we provide clear evidence of STAT1 overexpression in meningioma of different genotype and its correlation with an increased cellular proliferation. We demonstrate that STAT1 is aberrantly phosphorylated on both phosphosites, not because of the JAK/STAT pathway activation but because of the constitutive phosphorylation of EGFR, which elicits activation of the MAPK/ERK and PI3K/AKT pathways and an increase in the overall levels of Cyclin D1 and STAT1. Although the whole mechanism should be additionally studied to give a thorough understanding of the activating cascade and all the partners involved in it, our studies set the basis for re-evaluating EGFR inhibition in meningioma as possible therapeutic option.

Formatted: Indent: First line: 0"

References

1. Whittle IR, Smith C, Navoo P, Collie D. Meningiomas. *Lancet.* 2004; 363(9420):1535-1543.
2. Suppiah S, Nassiri F, Bi WL, et al. Molecular and translational advances in meningiomas. *Neuro Oncol.* 2019; 21(Supplement_1):i4-i17.
3. Bassiri K, Ferluga S, Sharma V, et al. Global Proteome and Phospho-proteome Analysis of Merlin-deficient Meningioma and Schwannoma Identifies PDLIM2 as a Novel Therapeutic Target. *EBioMedicine.* 2017; 16:76-86.
4. Dunn J, Ferluga S, Sharma V, et al. Proteomic analysis discovers the differential expression of novel proteins and phosphoproteins in meningioma including NEK9, HK2 and SET and deregulation of RNA metabolism. *EBioMedicine.* 2018.
5. Lee M, Rhee I. Cytokine Signaling in Tumor Progression. *Immune Netw.* 2017; 17(4):214-227.
6. Kiu H, Nicholson SE. Biology and significance of the JAK/STAT signalling pathways. *Growth Factors.* 2012; 30(2):88-106.
7. O'Shea JJ, Schwartz DM, Villarino AV, Gadina M, McInnes IB, Laurence A. The JAK-STAT pathway: impact on human disease and therapeutic intervention. *Annu Rev Med.* 2015; 66:311-328.
8. van de Veerdonk FL, Plantinga TS, Hoischen A, et al. STAT1 mutations in autosomal dominant chronic mucocutaneous candidiasis. *N Engl J Med.* 2011; 365(1):54-61.
9. Holland SM, DeLeo FR, Elloumi HZ, et al. STAT3 mutations in the hyper-IgE syndrome. *N Engl J Med.* 2007; 357(16):1608-1619.
10. You Z, Xu D, Ji J, Guo W, Zhu W, He J. JAK/STAT signal pathway activation promotes progression and survival of human oesophageal squamous cell carcinoma. *Clin Transl Oncol.* 2012; 14(2):143-149.
11. Tu Y, Zhong Y, Fu J, et al. Activation of JAK/STAT signal pathway predicts poor prognosis of patients with gliomas. *Med Oncol.* 2011; 28(1):15-23.
12. Lillemeier BF, Koster M, Kerr IM. STAT1 from the cell membrane to the DNA. *EMBO J.* 2001; 20(10):2508-2517.
13. Kohanbash G, Okada H. MicroRNAs and STAT interplay. *Semin Cancer Biol.* 2012; 22(1):70-75.
14. Ramana CV, Chatterjee-Kishore M, Nguyen H, Stark GR. Complex roles of Stat1 in regulating gene expression. *Oncogene.* 2000; 19(21):2619-2627.
15. Simpson JA, Al-Attar A, Watson NF, Scholefield JH, Ilyas M, Durrant LG. Intratumoral T cell infiltration, MHC class I and STAT1 as biomarkers of good prognosis in colorectal cancer. *Gut.* 2010; 59(7):926-933.
16. Chen G, Wang H, Xie S, Ma J, Wang G. STAT1 negatively regulates hepatocellular carcinoma cell proliferation. *Oncol Rep.* 2013; 29(6):2303-2310.
17. Sun Y, Yang S, Sun N, Chen J. Differential expression of STAT1 and p21 proteins predicts pancreatic cancer progression and prognosis. *Pancreas.* 2014; 43(4):619-623.
18. Schneckenleithner C, Bago-Horvath Z, Dolznig H, et al. Putting the brakes on mammary tumorigenesis: loss of STAT1 predisposes to intraepithelial neoplasias. *Oncotarget.* 2011; 2(12):1043-1054.
19. Meissl K, Macho-Maschler S, Muller M, Strobl B. The good and the bad faces of STAT1 in solid tumours. *Cytokine.* 2017; 89:12-20.
20. Hix LM, Karavitis J, Khan MW, Shi YH, Khazaie K, Zhang M. Tumor STAT1 transcription factor activity enhances breast tumor growth and immune suppression mediated by myeloid-derived suppressor cells. *J Biol Chem.* 2013; 288(17):11676-11688.
21. James MF, Lelke JM, Maccollin M, et al. Modeling NF2 with human arachnoidal and meningioma cell culture systems: NF2 silencing reflects the benign character of tumor growth. *Neurobiol Dis.* 2008; 29(2):278-292.
22. Hilton DA, Ristic N, Hanemann CO. Activation of ERK, AKT and JNK signalling pathways in human schwannomas in situ. *Histopathology.* 2009; 55(6):744-749.

Formatted: German (Germany)

23. Livak KJ, Schmittgen TD. Analysis of relative gene expression data using real-time quantitative PCR and the 2(-Delta Delta C(T)) Method. *Methods.* 2001; 25(4):402-408.

24. Ferluga S, Hantgan R, Goldgur Y, Himanen JP, Nikolov DB, Debinski W. Biological and structural characterization of glycosylation on ephrin-A1, a preferred ligand for EphA2 receptor tyrosine kinase. *J Biol Chem.* 2013; 288(25):18448-18457.

25. Puttmann S, Senner V, Braune S, et al. Establishment of a benign meningioma cell line by hTERT-mediated immortalization. *Lab Invest.* 2005; 85(9):1163-1171.

26. Schwechheimer K, Kartenbeck J, Moll R, Franke WW. Vimentin filament-desmosome cytoskeleton of diverse types of human meningiomas. A distinctive diagnostic feature. *Lab Invest.* 1984; 51(5):584-591.

27. Sorrell JM, Caplan AI. Fibroblasts-a diverse population at the center of it all. *Int Rev Cell Mol Biol.* 2009; 276:161-214.

28. Komohara Y, Horlad H, Ohnishi K, et al. M2 macrophage/microglial cells induce activation of Stat3 in primary central nervous system lymphoma. *J Clin Exp Hematop.* 2011; 51(2):93-99.

29. Seif F, Khoshmirsafa M, Aazami H, Mohsenzadegan M, Sedighi G, Bahar M. The role of JAK-STAT signaling pathway and its regulators in the fate of T helper cells. *Cell Commun Signal.* 2017; 15(1):23.

30. Mawrin C, Sasse T, Kirches E, et al. Different activation of mitogen-activated protein kinase and Akt signaling is associated with aggressive phenotype of human meningiomas. *Clin Cancer Res.* 2005; 11(11):4074-4082.

31. Qin HR, Kim HJ, Kim JY, et al. Activation of signal transducer and activator of transcription 3 through a phosphomimetic serine 727 promotes prostate tumorigenesis independent of tyrosine 705 phosphorylation. *Cancer Res.* 2008; 68(19):7736-7741.

32. Tong J, Taylor P, Moran MF. Proteomic analysis of the epidermal growth factor receptor (EGFR) interactome and post-translational modifications associated with receptor endocytosis in response to EGF and stress. *Mol Cell Proteomics.* 2014; 13(7):1644-1658.

33. Seshacharyulu P, Ponnusamy MP, Rachagani S, et al. Targeting EGF-receptor(s) - STAT1 axis attenuates tumor growth and metastasis through downregulation of MUC4 mucin in human pancreatic cancer. *Oncotarget.* 2015; 6(7):5164-5181.

34. Roskoski R, Jr. ErbB/HER protein-tyrosine kinases: Structures and small molecule inhibitors. *Pharmacol Res.* 2014; 87:42-59.

35. Yang J, Stark GR. Roles of unphosphorylated STATs in signaling. *Cell Res.* 2008; 18(4):443-451.

36. Moazzam AA, Wagle N, Zada G. Recent developments in chemotherapy for meningiomas: a review. *Neurosurg Focus.* 2013; 35(6):E18.

37. Brastianos PK, Horowitz PM, Santagata S, et al. Genomic sequencing of meningiomas identifies oncogenic SMO and AKT1 mutations. *Nat Genet.* 2013; 45(3):285-289.

38. Clark VE, Harmanci AS, Bai H, et al. Recurrent somatic mutations in POLR2A define a distinct subset of meningiomas. *Nat Genet.* 2016; 48(10):1253-1259.

39. Magrassi L, De-Fraja C, Conti L, et al. Expression of the JAK and STAT superfamilies in human meningiomas. *J Neurosurg.* 1999; 91(3):440-446.

40. Khodarev NN, Roizman B, Weichselbaum RR. Molecular pathways: interferon/stat1 pathway: role in the tumor resistance to genotoxic stress and aggressive growth. *Clin Cancer Res.* 2012; 18(11):3015-3021.

41. Sadzak I, Schiff M, Gattermeier I, et al. Recruitment of Stat1 to chromatin is required for interferon-induced serine phosphorylation of Stat1 transactivation domain. *Proc Natl Acad Sci U S A.* 2008; 105(26):8944-8949.

42. Petschnigg J, Groisman B, Kotlyar M, et al. The mammalian-membrane two-hybrid assay (MaMTH) for probing membrane-protein interactions in human cells. *Nat Methods.* 2014; 11(5):585-592.

43. Collins-McMillen D, Stevenson EV, Kim JH, et al. HCMV utilizes a non-traditional STAT1 activation cascade via signaling through EGFR and integrins to efficiently

Formatted: German (Germany)

Formatted: German (Germany)

promote the motility, differentiation, and polarization of infected monocytes. *J Virol.* 2017.

44. Smaill JB, Rewcastle GW, Loo JA, et al. Tyrosine kinase inhibitors. 17. Irreversible inhibitors of the epidermal growth factor receptor: 4-(phenylamino)quinazoline- and 4-(phenylamino)pyrido[3,2-d]pyrimidine-6-acrylamides bearing additional solubilizing functions. *J Med Chem.* 2000; 43(7):1380-1397.

45. Norden AD, Raizer JJ, Abrey LE, et al. Phase II trials of erlotinib or gefitinib in patients with recurrent meningioma. *J Neurooncol.* 2010; 96(2):211-217.

46. Conradt L, Godl K, Schaab C, et al. Disclosure of erlotinib as a multikinase inhibitor in pancreatic ductal adenocarcinoma. *Neoplasia.* 2011; 13(11):1026-1034.

47. Vanhatupa S, Ungureanu D, Paakkunainen M, Silvennoinen O. MAPK-induced Ser727 phosphorylation promotes SUMOylation of STAT1. *Biochem J.* 2008; 409(1):179-185.

48. Han W, Carpenter RL, Cao X, Lo HW. STAT1 gene expression is enhanced by nuclear EGFR and HER2 via cooperation with STAT3. *Mol Carcinog.* 2013; 52(12):959-969.

Figure Legends

Fig. 1 STAT1 and its phosphorylated forms are overexpressed in meningioma. **A** Representative WB analysis showing the expression of total and pSTAT1 in different grade meningiomas *vs.* NMT **B** Representative images showing the IHC staining of STAT1 and pSTAT1 in the three grades meningiomas compared to normal meninges (see black arrows) at 200X magnification. Mean scores are presented in the table below for the specimens and the normal controls examined (see also Supplementary Table 21 for the full list of specimens examined and the corresponding scores – n=47). **C** *STAT1* expression levels in WHO I (n=40), WHO II (n=25) and WHO III (n= 10) meningioma tumors normalised *vs.* normal meningeal tissue (NMT). Data are presented as mean ± SEM; * = p≤ 0.05. **D** WB showing pSTAT1 and STAT1 in normal brain (NB) and additional normal meninges (NMT-1 and NMT-2) compared to sample J6 (meningioma) as positive control. **E** Representative WB analysis of STAT1 and pSTAT1 in BM-1 and in WHO I MN cells (MNs) *vs.* HMC. **F** *STAT1* expression levels in BM-1 (n=4) and in MN cells (n=24) normalised *vs.* HMC. Data are presented as mean ± SEM; ** = p≤ 0.01. **E G** Confocal z-stack images showing the immunofluorescent staining of STAT1 (red) and pSTAT1 (Y701- green and S727- red) in MN cells *vs.* HMC. Scale bar 50 µm. Nuclei were stained with DAPI (blue).

Fig. 2 STAT1 phosphorylation in meningioma cells is not dependent on the JAK/STAT pathway. **A**WB of WHO I meningioma tumor tissue lysates (n=8); the presence of gamma interferon (IFNγ) and macrophage infiltration (CD163) into the tumor were analysed in relation to STAT1 and pSTAT1 levels. Phospho-JAK1 was used to detect activation of the JAK-STAT pathway (*=positive control for pJAK1 antibody. **B**). WB of total and pSTAT1 in BM-1 and HMC cells, grown in different culture condition. HMC: HMC cells media; MN: MN cells media; MN-SF: MN-serum free media; MN-SF+FBS: MN serum free for 24 h + FBS for 24h; MN Cond: meningioma cells-conditioned media**C** WB analysis of STAT1 and pSTAT1 protein levels in HMC and two primary MN cells after IFNγ treatment at the concentration of 50 ng/ml for the indicated amount of time. Phosho-JAK1 and pJAK2 are shown to confirm the activation of the JAK/STAT pathway. **D** Representative confocal images (z-stack) showing localization of pSTAT1-Y701 (green) and pSTAT1-S727 (red) in primary MN cells before and after IFNγ stimulation (50 ng/ml for 1 h). Scale bar 50 µm. Nuclei were stain with DAPI (blue). **E** WB analysis of SOCSs and PIASs protein levels in BM-1 and primary MNs compared to HMC.

Fig. 3 STAT1 overexpression increases meningioma cells proliferation. **A** Histogram representing the percentage of statistical reduction in STAT1 and Cyclin D1 protein levels after *STAT1* sh-RNA-mediated silencing using a pool of three shRNA in 3 primary MN cells compared to scramble; a representative WB is shown underneath. Data are presented as mean ± SD; *** = p≤ 0.001. **B** Percentage of reduction in *STAT1* expression associated to *STAT1* sh-RNA-mediated silencing compared to control shown in **A**; Data are presented as mean ± SEM; ** = p≤ 0.01. **C-D** Representative images of the immunofluorescent staining of STAT1 (green) and the proliferation marker Ki67 (red) (**D**) after *STAT1* sh-RNA-mediated silencing compared to scramble. Nuclei are stain with DAPI (blue). **E-F** Histogram presenting the statistical reduction of proliferating cells and total number of cells (**F**) after STAT1-KD compared to control. Data are presented as mean ± SD; *** = p≤ 0.001, ** = p≤ 0.01. **G** Representative WB, showing the reduction in AKT and ERK1/2 phosphorylation following STAT1 silencing. **H** Histogram representing the WB quantification of total and phosphorylated AKT and ERK1/2 following STAT1 silencing in 3 primary MN cells, *** = p≤ 0.001, ns= not significant.

Fig. 4 STAT1 activating mutations induce phosphorylation of AKT, ERK1/2 and an increased proliferation of U251-MG cells. **A** WB representing total and phosphorylated STAT1 levels in U251-MG compared to HMC and BM-1 cells. **B** WB showing overexpression of STAT1-WT and activating mutants in U251-MG cells and the related activation of pAKT and pERK1/2. **C** *STAT1* expression levels in U251-MG cells normalised *vs. STAT1* expression levels in pCDNA transfected cells ~~(=1)~~. Data are presented as mean ± SEM; *** = p≤ 0.001. **D** Histogram presenting the statistical increased in cell proliferation in U251-MG cells overexpressing the activating STAT1 mutants (STAT1-Y701F, STAT1-S727E, STAT1-Y701F/S727E). Data were normalised for STAT1-pCDNA-transfected cells and presented as FC of growth *vs.* STAT1-WT; *** = p≤ 0.001.

Fig. 5 The constitutive activation of the EGFR in meningioma induces STAT1 phosphorylation. **A** Representative WB analysis of total and pEGFR-Y1068 in meningioma, when compared to control. Upper panel: WHO I, II and III meningioma tissues compared to NMT; lower panel: BM-1 and primary MN cells compared to HMC. **B** WB of STAT1 and pSTAT1 protein levels after treatment with 5 μM of canertinib, afatinib and erlotinib in BM-1 cells. The reduced levels pEGFR-Y1068 confirmed drug activity. **C** ATP-proliferation assay performed in BM-1 cells after treatment with different concentrations of canertininb, afatinib and erlotinib for 24 h. **D** WB analysis of STAT1, pSTAT1 and other markers of proliferation in primary MN cells after treatment with 10 μM of canertininb. **E** Histograms representing WB quantification at 3 and 24 h for STAT1, pSTAT1, pAKT, pERK 1/2 and Cyclin D1 after canertininb treatment in three different primary MN cells (see Supplementary Fig. 4). Data are presented as mean ± SEM, *= p< 0.05; **= p< 0.01; ***= p< 0.001. **F** q-PCR analysis showing the statistical reduction of *STAT1* gene expression at 3, 6 and 24 h after treatment with 10 μM of canertininb (n=3). Data are presented as mean ± SEM; **= p< 0.01. **G** WB representing STAT1 and pSTAT1 in BM-1 cells, following treatment with EGF (50 ng/ml) for 5, 30 and 60 minutes.

NOA-D-19-00065R2

Constitutive activation of the EGFR-STAT1 axis increases proliferation of meningioma tumor cells

Sara Ferluga[1], Daniele Baiz[1], David A. Hilton[2], Claire L. Adams[1], Emanuela Ercolano[1], Jemma Dunn[1], Kayleigh Bassiri[1], Kathreena M. Kurian[3] and C. Oliver Hanemann[1, 4]

[1] University of Plymouth, Faculty of Health: Medicine, Dentistry and Human Sciences, The Institute of Translational and Stratified Medicine, The John Bull Building, Plymouth Science Park, Research Way, Plymouth UK, PL6 8BU

[2] Cellular and Anatomical Pathology, Plymouth Hospitals NH Trust, Derriford Road, Plymouth UK, PL6 8DH

[3] Department of Neuropathology, Pathology Sciences, Southmead Hospital, Southmead Road, Bristol UK, BS10 5NB

[4] **Corresponding author**: Prof. Clemens Oliver Hanemann MD, FRCP, Director of the Institute of Translational and Stratified Medicine, University of Plymouth, Faculty of Health: Medicine, Dentistry and Human Sciences, Plymouth Science Park, Research Way, Plymouth UK, PL6 8BU. Phone: +44 1752437418, Fax: +441752517846, E-mail: Oliver.Hanemann@plymouth.ac.uk

Running Title: EGFR-STAT1 tumor-promoting role in meningioma

Funding: This work was funded by Brain Tumour Research. DB was partially funded by the FP7 Marie Curie Actions (PCOFUND-GA-20126001). Tissue samples were obtained from University Hospitals Plymouth as part of the UK Brain Archive Information Network (BRAIN UK) which is funded by the Medical Research Council.

Conflict of Interest: Authors declare that there are no conflicts of interest.

Authorship: Designing and execution of most of the experiments, data interpretation, manuscript and figures preparation – SF

Designing and execution of gene expression studies, data interpretation, writing of the related part, performing experimental revisions and addressing comments to reviewers, proofreading of the manuscript – DB

Designing and execution of immunohistochemistry, data interpretation, writing of the related part – DAH

Designing and execution of the flow cytometry experiments, data interpretation, writing of the related part – CLA

Managing of tumor digestions and primary MN cells cultures – EE

Supporting with Western blot studies on MN Merlin status – JD

Supporting with the initial identification of STAT1 in meningioma – KB

Providing the majority of the samples involved in the study – KMK

Intellectual input to the critical design of the study, data interpretation, manuscript preparation - COH

Total Word Count: 6217

Abstract

Background: Meningiomas are the most frequent primary brain tumors of the central nervous system. The standard of treatment is surgery and radiotherapy, but effective pharmacological options are not available yet. The well-characterised genetic background stratifies these tumors in several subgroups, thus increasing diversification. We identified EGFR-STAT1 overexpression and activation as a common identifier of these tumors.

Methods: We analysed STAT1 overexpression and phosphorylation in 131 meningiomas of different grades and locations by utilising several techniques, including Western blots, qPCR and immunocytochemistry. We also silenced and overexpressed wild-type and mutant forms of the gene to assess its biological function and its network. Results were further validated by drug testing.

Results: STAT1 was found widely overexpressed in meningioma but not in the corresponding healthy controls. The protein showed a constitutive phosphorylation not dependent on the JAK/STAT pathway. *STAT1* knock-down resulted in a significant reduction of cellular proliferation and deactivation of AKT and ERK1/2. STAT1 is known to be activated by EGFR, so we investigated the tyrosine kinase and found that EGFR was also constitutively phosphorylated in meningioma and was responsible for the aberrant phosphorylation of STAT1. The pharmaceutical inhibition of EGFR caused a significant reduction in cellular proliferation and of overall levels of Cyclin D1, pAKT and pERK1/2.

Conclusions: STAT1 EGFR-dependent constitutive phosphorylation is responsible for a positive feedback loop that causes its own overexpression and consequently an increased proliferation of the tumor cells. These findings provide the rationale for further studies aiming to identify effective therapeutic options in meningioma.

Keywords: Meningioma, STAT1, EGFR, cancer, brain

Importance of the Study

Meningioma accounts for 37% of primary brain tumors. This year in the United States an estimated thirty-two thousand people will be diagnosed with meningioma. These tumors can cause mild to severe morbidity and even WHO grade I can have a more aggressive clinical course. Therapeutic options are still limited to surgical resection and radiotherapy since more effort is needed to decipher the communal molecular mechanisms that define meningiomas despite their genetic background.

Aiming to discover novel therapeutic targets, we identified STAT1 as aberrantly overexpressed and constitutively activated in most of the meningioma examined. Its activation is dependent on the constitutive phosphorylation of EGFR and leads to an increased proliferation of tumor cells. We show that specific EGFR inhibition can reduce tumor cell proliferation and we show evidence why previous trials failed. Therfore, we suggest that this therapeutic strategy be re-evaluated.

Introduction

Meningiomas are the most common primary brain tumors, classified meningiomas as Grade I (~80%), atypical Grade II (15-20%) and anaplastic/malignant Grade III (1-3%). Surgery is the primary choice of treatment; complete resection may be curative but it can be achieved only for permissive locations[1]. The genetic background of meningioma is well characterised, with inactivation/deletion of *NF2* found in ~60% of sporadic meningiomas[2].

Previously, we identified phosphorylated Signal Transducer and Activator of Transcription 1 (STAT1) as overexpressed in the grade I meningioma cell line [3] and phosphorylated STAT1 in meningioma tissue of all grades[4]. In addition, we identified phosphorylation of STAT3 among remaining STAT family members[3,4]. STAT1 belongs to the STAT protein family that comprise seven members (STAT1-4, STAT5A, STAT5B and STAT6), and it can be phosphorylated on the tyrosine 701 (Y701) and the serine 727 (S727)[5,6]. STATs are essential components of the evolutionarily conserved JAK/STAT signalling pathway[4,7] that plays a role in immune response[8,9] and its dysregulation is linked to cancer[10,11]. This canonical pathway is activated by ligands including interferons, interleukins and some growth factors, binding to their receptors thus inducing phosphorylation of the JAKs (Janus Kinases), leading to tyrosine-STAT phosphorylation by JAKs[4,6]. In addition STATs can also be phosphorylated by receptor tyrosine kinases and cytoplasmic non-receptor tyrosine kinases[5]. Phosphorylated STATs homo- and hetero-dimerize entering the nucleus to regulate transcription of target genes[6,12]. JAKs include JAK1-3 and TYK2. JAK1 and JAK2 are phosphorylated following type-II interferon (IFNγ) stimulation, while JAK1 and TYK2 are activated in type-I interferon signalling (IFNα, IFNβ; etc.)[4-6]. Activated JAK/STAT pathway can be quenched by the SOCSs (Suppressors Of Cytokine Signalling), the PIASs (Protein Inhibitors of Activated STAT) and the PTPs (Protein Tyrosine Phosphatases)[5]

Activated STAT1 acts as a transcriptional regulator, controlling its own transcription as well as the expression of several IFN-regulated genes (IRGs)[13,14]. STAT1 was considered a tumor suppressor as its expression correlated with good prognosis in several types of cancer[15-18]. However, other studies established a pro-tumorigenic role of STAT1, which correlated with its overexpression and activation[19]. Due to its function in sensing and regulating cytokine production, STAT1 exerts a role in promoting an immunosuppressive tumor environment[19,20]. Hence, the overall role of STAT1 in cancer remains complex suggesting that its function is most likely cancer type-dependent.

In the present study, we identified STAT1 as overexpressed and phosphorylated in meningioma compared to normal and we show that its overexpression correlates with an increased proliferation of the tumor cells as well as an activation of AKT and ERK1/2. We demonstrate that STAT1 overexpression and phosphorylation is not dependent on the JAK/STAT pathway but it depends on a positive feedback loop caused by the constitutive activation of the Epidermal Growth Factor Receptor (EGFR). The pharmaceutical inhibition of EGFR in meningioma caused the deactivation of STAT1 and other cancer-related pathways, eventually leading to a significant reduction in cellullar proliferation. Our findings underline a crucial role of the EGFR and STAT1 signalling in the pathology of meningiomas and point to a therapeutic potential of its inhibition.

Materials and Methods

Meningioma specimens, tumor digestion and primary meningioma cultures

Meningioma specimens were collected following the ethical approvals received a unique MN number (Supplementary Table 1). Normal meningeal tissue (NMT) was purchased from Analytical Biological Service Inc.

Primary cells were generated from 36 fresh tumor tissue. Tissue were disaggregated in DMEM with 15% FBS, 100 U/ml penicillin/streptomycin and 20 U/ml Collagenase III (Worthington Biochemical Corp) for 2 h at 37 °C; after cells were pelleted at 1000 rpm for 5 min, resuspended and seeded (modified from[21]). MN cells were cultured in DMEM at 37 °C in 5% CO2. HMC cells (Caltag Medsystems Ltd) were grown in the recommended medium at 37 °C in 5% CO_2. Cells were kept on average 4-5 passages.

Normal human meningeal cell were purchased from ScienceCell (UK distributor: Caltag Medsystems; Catalog#1400), U251 glioma cells were purchased from ECACC (Cat n.: 09063001), an immortalized grade 1 meningioma cell line BM-1 were (DSMZ; Cat.n.: ACC 599) and authenticated via genomic fingerprinting (Eurofins Genomics Europe Applied Genomics GmbH).

Western blotting, immunofluorescence and immunohistochemistry

Western blots (WB) from 26 frozen tissues and cell cultures were performed as previously described[3]. All primary antibodies used are listed in Supplementary Table 2. Immunoreactive bands were quantified using Scion Image software and each band was normalized *vs.* the corresponding GAPDH.

Immunofluorescence of 38 paraffin embedded tissue was performed as previously described[3]. Confocal microscopy was executed using a Leica DMI6000B; Z-stack micrographs were taken using the 40X or

63X objectives. Immunofluorescent images for STAT1-silencing studies were taken with the Olympus CKX41 with the 20X objective; images were processed with the QCapture Pro 6.0 software.

For immunohistochemistry, paraffin sections (4μm) were processed as described[22]. Avidin-biotin blocking solution was used with EDTA pretreatment. Sections were incubated with appropriate biotin-labelled secondary antibody and with horseradish peroxidase for detection using Vectashield Elite (Vector Laboratories UK) according to the manufacturer's protocol. As a control, sections were incubated with omission of the primary antibody.

Results were reviewed 'blind' to the histological grade by a neuropathologist (DAH). Semiquantitaive assessment of the intensity of immunoreactivity was undertaken and scored as follow: 0 none; 1 weak; 2 moderate; 3 strong.

RNA isolation and gene expression analysis

Total RNA was extracted from 95 frozen tissues and cells using the Qiazol® reagent (Qiagen UK), following manufacturer's protocol. The quality, integrity and concentration of RNA were established using the NanoDrop ND-2000 (ThermoFisher Scientific UK).

Real-Time PCR (qPCR) was conducted using 50 ng/well employing the EXPRESS One-Step SYBR® GreenERTM kit (Invitrogen) on a LightCycler® 480 System (Roche Diagnostics, Switzerland), following manufacturer's protocol (primers annealing temperature= 58 °C). Primers used were: PrimePCR™ SYBR® Green Assay STAT1 (BioRad), hGAPDH (2 μM, Invitrogen- Forward: 5'-GAGAAGGCTGGGGCTCATTT-3'; Reverse 5'-AGTGATGGCATGGACTGTGG-3'). Relative gene expression analysis of STAT1 and GAPDH was calculated using the $2^{-\Delta\Delta Ct}$ method[23], employing the HMC as calibrator.

STAT1 silencing and overexpression

Stat1 shRNA Lentiviral Particles (Santa Cruz Biotechnology, sc-44123-V), containing 3 target-specific constructs that encode 19-25nt (plus hairpin) or scramble shRNA control (Santa Cruz Biotechnology, sc-108080), were added onto the cells in media containing protamine sulfate salt (8 μg/ ml) (Sigma). Cells were infected for 48 h before applying puromycin (5 μg/ml) for 3 days.

STAT1-WT gene was cloned into pCDNA3.1+ in a two-step process using the following primers: STAT1-F1 (5'-AAAGCTAGCGGCCGGCCATGTCTCAG-3'), STAT1-R1 (5'-CGTCTCGAGGTCAATTACCAAACCAGGCT-3') for the first part; STAT1-2F (5'-GACCTCGAGACGACCTCTCT), STAT1-2R (5'-AGTGTTTAAACTTAATTAACTATACTGTGTTCA-3') for the second part. The 551 bp long STAT1 part in between the restriction sites HindIII and EcoRI was synthesised (GeneArt, ThermoFisher Scientific) to generate the following mutations: Y701F, S727E and

Y701F/S727E; each one was cloned into pCDNA-STAT1-WT to replace the wild-type part. All generated plasmids were sequenced before further use (Eurofins). U251-MG cells were transfected and selected as previously described [24].

Ki-67 staining and Proliferation assay

For Ki-67 staining, cells were grown on chamber slides, lentivirus-transfected and stained as previously described[3].

For U251-MG proliferation assay, the pool of U251-MG selected cells, transfected with pCDNA, STAT1-WT and the three mutants, were seeded at 1000 cell/well in 96 well plates and proliferation was determined after 24, 48 and 72 h using the 'CellTiter-Glo® Luminescent Cell Viability Assay' as recommended by the supplier (Promega).

For drug testing, meningioma cells (~3000 cell/well) were plated in 96-well culture plates and allowed to proliferate for 24 h. Cell proliferation was calculated as percentage of control cells. Graphs were generated using GraphPad Prism 5.

Flow cytometry analysis

Confluent meningioma cells were resuspended in ice-cold staining buffer (PBS, 2%FBS) at a final concentration of $1x10^5$ cells. Cells were stained for 30 min at RT in the dark with the following: CD45-FITC, HLA-DR-PE, CD14-PerCP5.5 and CD44 –APC (Becton Dickinson Biosciences, Pharmigen), washed twice with 2 ml of staining buffer and centrifuged at 1500 rpm for 5 min at 4°C . The relevant single isotype controls were used. Data acquisition was collected on $1x10^4$ cells on a Accuri flow cytometer (BD Biosciences) and analysis was performed using the Flow Jo software v10.0 (FlowJo LLC, Ashland, OR).

Statistical analysis

Probability (p) values were calculated using the Student's t-Test or the ANOVA one-way analysis of variance, using GraphPad Prism 5.01 and MS Excel 2016 software. P values <0.05 were considered statistically significant. The results are expressed as means ± SD or ± SEM.

Results

STAT1 is overexpressed and aberrantly activated in meningioma

We analysed STAT1 expression in meningioma tumors compared to normal meninges (NMT). In all cases STAT1 was overexpressed and in most of the cases, we detected high levels of phosphorylated STAT1 (Y701 and S727) (representative Western blot of Fig. 1A and qPCR of Fig. 1C). Immunohistochemical studies validated STAT1 overexpression in all meningioma samples (Fig. 1B); also pSTAT1-Y701 and -S727 showed higher staining compared to normal meninges and an increasing score throughout the grades. As control, we further analysed STAT1 and pSTAT1 abundance in two additional normal meninges and a normal brain (Fig. 1D).

Then, we examined STAT1 expression and phosphorylation in meningioma-derived primary cells (MN) and in BM-1[25] compared to HMC. MN cells were used between passage 3 and 5 and no B/T lymphocytes or infiltrating macrophages were detected (Supplementary Fig. 1A). All cells were vimentin-positive[26] and CD90-negative, suggesting no fibroblasts contamination[27] (Supplementary Fig. 1B). STAT1 was found overexpressed in BM-1 and MNs compared to HMC and both pSTAT1-Y701 and -S727 were present across all samples while faint and undetectable in HMC (Fig. 1C). Q-PCR analysis confirmed that *STAT1* expression was higher in most of the MNs and in BM-1 compared to control (Fig. 1F). Of note, STAT1 overexpression was independent of Merlin status (Supplementary Fig. 1C, D).

Furthermore, pSTAT1-Y701 showed a cytoplasmic localization while pSTAT1-S727 was nuclear (Fig. 1B), in agreement with the immunofluorescent staining of primary MN cells (Fig. 1G).

Overall, we examined 131 meningiomas *vs.* 10 normal meninges and 5 normal brains and we demonstrate substantial overexpression of STAT1 in 100 of them with a variety of methods (Supplementary Table 1).

STAT1 constitutive phosphorylation is not dependent on the JAK/STAT pathway

To further investigate STAT1 phosphorylation in the context of the tumor environment, we examined meningioma tumor lysates for the presence of interferon gamma (IFNγ) and tumor-associated macrophages by using CD163 marker staining preferentially M2 macrophages [28]. Variable protein

levels of IFNγ and CD163 were detected, but there was no evident correlation with STAT1 phosphorylation and no JAK1 phosphorylation was detected (Fig 2A).

STAT1 usually becomes phosphorylated as a result of JAK/STAT pathway activation in response to external stimuli[6]. We examined whether STAT1 overexpression and phosphorylation was dependent on the culture conditions and secreted factors. Culturing HMC in serum-free (SF) media and in BM-1 conditioned media, and BM-1 in SF media, we confirmed that STAT1 overexpression and phosphorylation was not due to external factors, but most likely to an intrinsic activation (Fig. 2B).

Next, we decided to test the ability of the JAK/STAT pathway to respond to activating stimuli in meningioma cells. HMC and two MNs were treated with IFNγ; in HMC, JAK1 and JAK2 activated within 10 min after treatment as well as pSTAT1-Y701 whilst pSTAT1-S727 phosphorylated within 1 h. The same behaviour was observed in MNs confirming that the JAK/STAT pathway was functional; however, STAT1 was constitutively phosphorylated in non-treated cells while pJAK1 and pJAK2 were not (Fig. 2C). The same experiment, performed using interferon alpha (IFNα), produced comparable results (Supplementary Fig. 2A).

After activation, pSTAT1 is known to dimerize and translocate into the nucleus[6]. IFNγ treatment was indeed able to induce pSTAT1-Y701 nuclear internalization (Fig. 2D, Supplementary Fig. 2B). Thus, the JAK/STAT1 pathway can be activated *via* IFN in meningioma cells but there was also an IFN-independent intrinsic activation.

STAT1 constitutive phosphorylations could be due to a deficient deactivation of the pathway[4,5,29]. Thus, we analysed the levels of the SOCSs and the PIASs in HMC, BM-1 and MN cells (Fig. 2E), which did not correlate with the constitutive phosphorylation of STAT1 observed in these samples (Fig. 1E).

Overall, these data suggest that the JAK/STAT pathway is functional but not over-activated. Therefore, we hypothesized other mechanisms must be involved in maintaining STAT1 in a constitutive phosphorylated form in the meningioma samples analyzed.

STAT1 overexpression is associated with an increased proliferation of meningioma cells

To investigate the biological significance of STAT1 overexpression in meningioma we silenced the protein in MN cells. Lentiviral-mediated shRNA delivery into the cells produced an over 70% reduction in protein expression (Fig. 3A) and a 50% reduction in gene expression levels compared to scramble (Fig. 3B). STAT1-silenced cells displayed a reduction in STAT1 immunofluorescent staining as well as

a reduction in Ki67-positive cells (Fig. 3C). Proliferating cells were reduced from ~22% to less than 5% in MNs (Fig. 3D, E). This was in agreement with the reduction of the total number of cells (Fig. 3F) and a 40% reduction of Cyclin D1 (Fig. 3A). A similar effect was observed in BM-1 cells (Supplementary Fig. 3A-D). Taken together, our results demonstrate that STAT1 overexpression is associated to an increased proliferation of meningioma tumor cells.

The MAPK-ERK and the AKT pathways are known to be active in meningioma and to influence tumor progression[30]. After STAT1-KD, both AKT and ERK1/2 showed a 95% and 80% reduction in protein phosphorylation respectively (Fig. 3G, H), supporting a critical involvement of STAT1 in the activation of pro-proliferative pathways.

Phosphorylated STAT1 affects activation of AKT and ERK1/2 and cellular proliferation

We used phosphomimetics to further characterise the effects of STAT1 phosphorylation. Phenylalanine (F) and Glutamic acid (E) are used to mimic the structure of a phosphorylated tyrosine (Y) and phosphorylated serine (S) respectively[31]. We produced three different STAT1 mutants: Y701F, S727E and the double mutant Y701F/S727E. Since STAT1 is constitutively phosphorylated in meningioma, we used U251-MG cells as a model because this cell line showed levels of total and pSTAT1 lower than HMC (Fig. 4A). STAT1 overexpression in U251-MG for wild-type (WT) and mutants was confirmed by WB and qPCR (Fig. 4B, C). STAT1 overexpression in U251-MG cells determined an increased phosphorylation of AKT and ERK1/2, where the effect was particularly evident for pERK1/2 in STAT1-S727E and STAT1-Y701F/S727E mutants (Fig. 4B).

The proliferation of transfected cells was measured over a period of 72 h and normalised for the empty-vector control. All STAT1 mutants showed a significantly increased proliferation rate compared to STAT1-WT; interestingly, the double mutant STAT1- Y701F/S727E, which represents STAT1 in its maximal activated condition, determined the highest pro-proliferative effect in U251-MG cells (Fig. 4B, 4D).

These experiments confirmed that the constitutive phosphorylation of STAT1 on both phosphosites affects the activation of the AKT and ERK1/2 pathways as well as the proliferation of the cells in agreement with STAT1 knock-down results in meningioma.

EGFR constitutive phosphorylation is responsible for STAT1 overexpression and activation

It has been previously shown that STAT1 can be phosphorylated by EGFR, a key tyrosine kinase relevant to the majority of tumors[32,33]. We examined the EGFR status in meningioma tissues and cells,

detecting high levels of pEGFR in both tumor lysates and meningioma cells, when compared to normal meningeal tissue (NMT) and HMC (Fig. 5A).

To test whether the constitutive phosphorylation of EGFR was responsible for STAT1 phosphorylation, we treated BM-1 cells with three different EGFR inhibitors (canertinib andafatinib, 2nd generation irreversible inhibitors) and erlotinib (1st generation, reversible inhibitor), , for 30 min, 3, 6 and 24 h[34]. Canertinib (and similarly afatinib) decreased STAT1 expression of about 60% within 24 h upon; pSTAT1-Y701 was almost abolished 30 min after treatment but was restored at 24 h while pSTAT1-S727 showed a decrease of about 90% compared to vehicle at 24 h (Fig. 5B). Almost no effect on total and pSTAT1 was detected after treatment with erlotinib, which did not cause an evident decrease in pEGFR-Y1068 after treatment (Fig. 5B).

EGFR blockade *via* canertinib and afatinib decreased pSTAT1 levels and determined a concentration-dependent decrease of cellular proliferation already at 24 h after treatment (Fig. 5C), with erlotinib being ineffective.

Since canertinib showed the strongest effect on STAT1 in BM-1 cells, we tested its effects on primary MNs (Fig. 5D). Canertinib was active in reducing EGFR constitutive phosphorylation in MN cells, reducing p-STAT1 levels after canertinib treatment; pSTAT1-S727 reduced of 65% already 3 h after treatment and stayed low over the 24 h; phosphorylated STAT1-Y701 also showed about 50% reduction 3 h after treatment and recovered between 6 and 24 h (Fig. 5D, E Supplementary Fig. 4).

Phospho-AKT and pERK1/2 showed a decrease of about 70% and Cyclin D1 reduced t0 50% in 24 h (Fig. 5D,E,Supplementary Fig. 4).

We wanted to examine whether the inhibition of pEGFR and thus of pSTAT1 had any effect on *STAT1* expression, as STAT1 is known to regulate its own transcription[35]. *STAT1* expression levels reduced by ~50% 24 h after treatment with canertinib in MNs (Fig. 5F), consistently with a 30% reduction in protein level observed by WB analysis (Fig. 5D, E, Supplementary Fig. 4).

Lastly, to confirm the link between EGFR activation and STAT1 phosphorylation, we treated BM-1 cells with the Epidermal Growth Factor (EGF) for 5, 30 and 60 minutes. Upon EGF treatment STAT1 was phosphorylated on Y701 within 5 minutes and on S727 within 30 minutes (Fig. 5G).

Hence, we showed that EGFR is responsible for STAT1 overexpression and constitutive activation in meningioma, which consequently increases proliferation of the tumor cells.

Discussion

Meningiomas are the most common primary brain tumor but there are no therapeutic options available other than surgery and radiotherapy[1,36]. The well-defined genetic background of meningioma is leading towards an increasing stratification of these tumors into subtypes[37,38]; however, common features should still be investigated.

We identified STAT1 as overexpressed and activated in 84% of meningioma examined. The only study exploring the expression levels of STAT and JAK superfamilies in meningiomas was published in 1999 showing higher immunoreactivity of JAK1 (see also Supplementary Fig. 2C), JAK2 and the STATs in meningiomas compared to normal dura[39]. Our data confirmed the expression of the JAKs in MN cells and in HMC; we showed that the JAK/STAT pathway is activated by IFNα and IFNγ, inducing nuclear localization of pSTAT1 as seen before[39]. As previously reported[40], activation of STAT1 after INFγ stimulation occurs via JAK kinases by phosphorylation on Y701, resulting in pSTAT1 translocation into the nucleus and subsequent phosphorylation at S727[41]. Double phosphorylation is required for maximal STAT1 activity. However, we show that STAT1 is constitutively phosphorylated in MNs but not in HMC, even without IFN stimulation and in serum-free conditions. In tumor lysates, STAT1 phosphorylation was not consistent with the presence of M2-polarised macrophages or IFNγ suggesting that the constitutive activation of STAT1 was not related to the JAK/STAT pathway.

To better understand the meaning of this STAT1 phosphorylation we used phosphomimetics, generating STAT1-Y701F, STAT1-S727E and STAT1-Y701F/S727E mutants. The overexpression of these mutants induced activation of two central nodes in cancer signalling, AKT and ERK1/2, and increased cellular proliferation. A similar approach was used on STAT3 in human prostate cancer cell, where the mutant STAT3-Y705F/S727E promoted survival, growth and invasion. They showed that the mutation S727E was increasing the transcription of c-Myc, which is an essential activator of cell growth

and proliferation[31]. It is very likely that a similar mechanism is happening also in meningioma, where STAT1-S727 showed a predominant nuclear localization exerting its role of transcriptional regulator.

We also showed the link between STAT1 overexpression and the increased proliferation of the tumor cells. This effect is most likely linked to an activating cascade involving ERK1/2 and AKT, since their activated state and cell proliferation were almost aborted after STAT1 silencing. The activation of the MAPK pathway is involved in both proliferation and apoptosis in meningioma[30], and we recently published a proteomic profiling of meningioma, identifying the aberrant activation of the PI3K/AKT pathway across all meningioma grades[4].

Aiming to identify the kinase responsible for STAT1 activation, we examined the status of EGFR, a tyrosine kinase able to phosphorylate STAT1[33,42,43]. EGFR was overexpressed and constitutively phosphorylated on Y1068 in all of the MN cells examined but not in HMC. To test whether EGFR phosphorylation was responsible for the constitutive activation of STAT1 we used three specific EGFR inhibitors canertinib, afatinib and erlotinib[44]. Whilst canertinib and afatinib, had a similar effect in reducing STAT1 phosphorylation on both phosphosites as well as on cell proliferation and viability, erlotinib, did not produce any significant effect. Interestingly this result is consistent with the unsuccessful clinical trial of erlotinib on recurrent meningiomas[45]. Erlotinib is a first generation ATP dependent reversible rather broad inhibitor[46], Afinitinib and Canertinib are non reversible second generation with high pEC50 https://www.proteomicsdb.org/#analytics/selectivity

In MN cells, canertinib (and afatinib) caused the de-phosphorylation of STAT1-Y701 and S&27 within 6and 24H respectively. Similarly, EGF stimulation induces an immediate and direct phosphorylation on Y701 and a later one on S727, suggesting the activation of an additional kinase downstream of EGFR, which is probably part of the MAPK/ERK1/2 pathway[47]. Indeed previous studies in pancreatic cancer demonstrated the relationship between EGFR and the downstream signalling regulators like pAKT, pERK1/2 and Cyclin D1[33]. In agreement, after canertinib treatment and after STAT1 silencing, we observed a significant reduction of pAKT and pERK1/2. Overall, levels of Cyclin D1 also displayed a significant reduction, consistently with the reduction in proliferation observed after STAT1 silencing and canertinib treatment.

The observed reduction in STAT1 expression suggest a feedback regulatory mechanism of pSTAT1 on its own promoter, already documented[35], as well as an EGFR/HER2-dependent regulation as previously shown in glioblastoma and breast cancer cell lines[48].

In conclusion, we provide clear evidence of STAT1 overexpression in meningioma of different genotype and its correlation with an increased cellular proliferation. We demonstrate that STAT1 is aberrantly

phosphorylated on both phosphosites, not because of the JAK/STAT pathway activation but because of the constitutive phosphorylation of EGFR, which elicits activation of the MAPK/ERK and PI3K/AKT pathways and an increase in the overall levels of Cyclin D1 and STAT1. Although the whole mechanism should be additionally studied to give a thorough understanding of the activating cascade and all the partners involved in it, our studies set the basis for re-evaluating EGFR inhibition in meningioma as possible therapeutic option.

References

1. Whittle IR, Smith C, Navoo P, Collie D. Meningiomas. *Lancet.* 2004; 363(9420):1535-1543.

2. Suppiah S, Nassiri F, Bi WL, et al. Molecular and translational advances in meningiomas. *Neuro Oncol.* 2019; 21(Supplement_1):i4-i17.

3. Bassiri K, Ferluga S, Sharma V, et al. Global Proteome and Phospho-proteome Analysis of Merlin-deficient Meningioma and Schwannoma Identifies PDLIM2 as a Novel Therapeutic Target. *EBioMedicine.* 2017; 16:76-86.

4. Dunn J, Ferluga S, Sharma V, et al. Proteomic analysis discovers the differential expression of novel proteins and phosphoproteins in meningioma including NEK9, HK2 and SET and deregulation of RNA metabolism. *EBioMedicine.* 2018.

5. Lee M, Rhee I. Cytokine Signaling in Tumor Progression. *Immune Netw.* 2017; 17(4):214-227.

6. Kiu H, Nicholson SE. Biology and significance of the JAK/STAT signalling pathways. *Growth Factors.* 2012; 30(2):88-106.

7. O'Shea JJ, Schwartz DM, Villarino AV, Gadina M, McInnes IB, Laurence A. The JAK-STAT pathway: impact on human disease and therapeutic intervention. *Annu Rev Med.* 2015; 66:311-328.

8. van de Veerdonk FL, Plantinga TS, Hoischen A, et al. STAT1 mutations in autosomal dominant chronic mucocutaneous candidiasis. *N Engl J Med.* 2011; 365(1):54-61.

9. Holland SM, DeLeo FR, Elloumi HZ, et al. STAT3 mutations in the hyper-IgE syndrome. *N Engl J Med.* 2007; 357(16):1608-1619.

10. You Z, Xu D, Ji J, Guo W, Zhu W, He J. JAK/STAT signal pathway activation promotes progression and survival of human oesophageal squamous cell carcinoma. *Clin Transl Oncol.* 2012; 14(2):143-149.

11. Tu Y, Zhong Y, Fu J, et al. Activation of JAK/STAT signal pathway predicts poor prognosis of patients with gliomas. *Med Oncol.* 2011; 28(1):15-23.

12. Lillemeier BF, Koster M, Kerr IM. STAT1 from the cell membrane to the DNA. *EMBO J.* 2001; 20(10):2508-2517.

13. Kohanbash G, Okada H. MicroRNAs and STAT interplay. *Semin Cancer Biol.* 2012; 22(1):70-75.

14. Ramana CV, Chatterjee-Kishore M, Nguyen H, Stark GR. Complex roles of Stat1 in regulating gene expression. *Oncogene.* 2000; 19(21):2619-2627.

15. Simpson JA, Al-Attar A, Watson NF, Scholefield JH, Ilyas M, Durrant LG. Intratumoral T cell infiltration, MHC class I and STAT1 as biomarkers of good prognosis in colorectal cancer. *Gut.* 2010; 59(7):926-933.

16. Chen G, Wang H, Xie S, Ma J, Wang G. STAT1 negatively regulates hepatocellular carcinoma cell proliferation. *Oncol Rep.* 2013; 29(6):2303-2310.

17. Sun Y, Yang S, Sun N, Chen J. Differential expression of STAT1 and p21 proteins predicts pancreatic cancer progression and prognosis. *Pancreas.* 2014; 43(4):619-623.

18. Schneckenleithner C, Bago-Horvath Z, Dolznig H, et al. Putting the brakes on mammary tumorigenesis: loss of STAT1 predisposes to intraepithelial neoplasias. *Oncotarget.* 2011; 2(12):1043-1054.

19. Meissl K, Macho-Maschler S, Muller M, Strobl B. The good and the bad faces of STAT1 in solid tumours. *Cytokine.* 2017; 89:12-20.

20. Hix LM, Karavitis J, Khan MW, Shi YH, Khazaie K, Zhang M. Tumor STAT1 transcription factor activity enhances breast tumor growth and immune suppression mediated by myeloid-derived suppressor cells. *J Biol Chem.* 2013; 288(17):11676-11688.

21. James MF, Lelke JM, Maccollin M, et al. Modeling NF2 with human arachnoidal and meningioma cell culture systems: NF2 silencing reflects the benign character of tumor growth. *Neurobiol Dis.* 2008; 29(2):278-292.

22. Hilton DA, Ristic N, Hanemann CO. Activation of ERK, AKT and JNK signalling pathways in human schwannomas in situ. *Histopathology.* 2009; 55(6):744-749.

23. Livak KJ, Schmittgen TD. Analysis of relative gene expression data using real-time quantitative PCR and the 2(-Delta Delta C(T)) Method. *Methods.* 2001; 25(4):402-408.

24. Ferluga S, Hantgan R, Goldgur Y, Himanen JP, Nikolov DB, Debinski W. Biological and structural characterization of glycosylation on ephrin-A1, a preferred ligand for EphA2 receptor tyrosine kinase. *J Biol Chem.* 2013; 288(25):18448-18457.

25. Puttmann S, Senner V, Braune S, et al. Establishment of a benign meningioma cell line by hTERT-mediated immortalization. *Lab Invest.* 2005; 85(9):1163-1171.

26. Schwechheimer K, Kartenbeck J, Moll R, Franke WW. Vimentin filament-desmosome cytoskeleton of diverse types of human meningiomas. A distinctive diagnostic feature. *Lab Invest.* 1984; 51(5):584-591.

27. Sorrell JM, Caplan AI. Fibroblasts-a diverse population at the center of it all. *Int Rev Cell Mol Biol.* 2009; 276:161-214.

28. Komohara Y, Horlad H, Ohnishi K, et al. M2 macrophage/microglial cells induce activation of Stat3 in primary central nervous system lymphoma. *J Clin Exp Hematop.* 2011; 51(2):93-99.

29. Seif F, Khoshmirsafa M, Aazami H, Mohsenzadegan M, Sedighi G, Bahar M. The role of JAK-STAT signaling pathway and its regulators in the fate of T helper cells. *Cell Commun Signal.* 2017; 15(1):23.

30. Mawrin C, Sasse T, Kirches E, et al. Different activation of mitogen-activated protein kinase and Akt signaling is associated with aggressive phenotype of human meningiomas. *Clin Cancer Res.* 2005; 11(11):4074-4082.

31. Qin HR, Kim HJ, Kim JY, et al. Activation of signal transducer and activator of transcription 3 through a phosphomimetic serine 727 promotes prostate tumorigenesis independent of tyrosine 705 phosphorylation. *Cancer Res.* 2008; 68(19):7736-7741.

32. Tong J, Taylor P, Moran MF. Proteomic analysis of the epidermal growth factor receptor (EGFR) interactome and post-translational modifications associated with receptor endocytosis in response to EGF and stress. *Mol Cell Proteomics.* 2014; 13(7):1644-1658.

33. Seshacharyulu P, Ponnusamy MP, Rachagani S, et al. Targeting EGF-receptor(s) - STAT1 axis attenuates tumor growth and metastasis through downregulation of MUC4 mucin in human pancreatic cancer. *Oncotarget.* 2015; 6(7):5164-5181.

34. Roskoski R, Jr. ErbB/HER protein-tyrosine kinases: Structures and small molecule inhibitors. *Pharmacol Res.* 2014; 87:42-59.

35. Yang J, Stark GR. Roles of unphosphorylated STATs in signaling. *Cell Res.* 2008; 18(4):443-451.

36. Moazzam AA, Wagle N, Zada G. Recent developments in chemotherapy for meningiomas: a review. *Neurosurg Focus.* 2013; 35(6):E18.

37. Brastianos PK, Horowitz PM, Santagata S, et al. Genomic sequencing of meningiomas identifies oncogenic SMO and AKT1 mutations. *Nat Genet.* 2013; 45(3):285-289.

38. Clark VE, Harmanci AS, Bai H, et al. Recurrent somatic mutations in POLR2A define a distinct subset of meningiomas. *Nat Genet.* 2016; 48(10):1253-1259.

39. Magrassi L, De-Fraja C, Conti L, et al. Expression of the JAK and STAT superfamilies in human meningiomas. *J Neurosurg.* 1999; 91(3):440-446.

40. Khodarev NN, Roizman B, Weichselbaum RR. Molecular pathways: interferon/stat1 pathway: role in the tumor resistance to genotoxic stress and aggressive growth. *Clin Cancer Res.* 2012; 18(11):3015-3021.

41. Sadzak I, Schiff M, Gattermeier I, et al. Recruitment of Stat1 to chromatin is required for interferon-induced serine phosphorylation of Stat1 transactivation domain. *Proc Natl Acad Sci U S A.* 2008; 105(26):8944-8949.

42. Petschnigg J, Groisman B, Kotlyar M, et al. The mammalian-membrane two-hybrid assay (MaMTH) for probing membrane-protein interactions in human cells. *Nat Methods.* 2014; 11(5):585-592.

43. Collins-McMillen D, Stevenson EV, Kim JH, et al. HCMV utilizes a non-traditional STAT1 activation cascade via signaling through EGFR and integrins to efficiently

promote the motility, differentiation, and polarization of infected monocytes. *J Virol.* 2017.

44. Smaill JB, Rewcastle GW, Loo JA, et al. Tyrosine kinase inhibitors. 17. Irreversible inhibitors of the epidermal growth factor receptor: 4-(phenylamino)quinazoline- and 4-(phenylamino)pyrido[3,2-d]pyrimidine-6-acrylamides bearing additional solubilizing functions. *J Med Chem.* 2000; 43(7):1380-1397.

45. Norden AD, Raizer JJ, Abrey LE, et al. Phase II trials of erlotinib or gefitinib in patients with recurrent meningioma. *J Neurooncol.* 2010; 96(2):211-217.

46. Conradt L, Godl K, Schaab C, et al. Disclosure of erlotinib as a multikinase inhibitor in pancreatic ductal adenocarcinoma. *Neoplasia.* 2011; 13(11):1026-1034.

47. Vanhatupa S, Ungureanu D, Paakkunainen M, Silvennoinen O. MAPK-induced Ser727 phosphorylation promotes SUMOylation of STAT1. *Biochem J.* 2008; 409(1):179-185.

48. Han W, Carpenter RL, Cao X, Lo HW. STAT1 gene expression is enhanced by nuclear EGFR and HER2 via cooperation with STAT3. *Mol Carcinog.* 2013; 52(12):959-969.

Figure Legends

Fig. 1 STAT1 and its phosphorylated forms are overexpressed in meningioma. **A** Representative WB analysis showing the expression of total and pSTAT1 in different grade meningiomas *vs.* NMT **B** Representative images showing the IHC staining of STAT1 and pSTAT1 in the three grades meningiomas compared to normal meninges (see black arrows) at 200X magnification. Mean scores are presented in the table below for the specimens and the normal controls examined (see also Supplementary Table 1 for the full list of specimens examined and the corresponding scores – n=47). **C** *STAT1* expression levels in WHO I (n=40), WHO II (n=25) and WHO III (n= 10) meningioma tumors normalised *vs.* normal meningeal tissue (NMT). Data are presented as mean ± SEM; * = p≤ 0.05. **D** WB showing pSTAT1 and STAT1 in normal brain (NB) and additional normal meninges (NMT-1 and NMT-2) compared to sample J6 (meningioma) as positive control. **E** Representative WB analysis of STAT1 and pSTAT1 in BM-1 and in WHO I MN cells (MNs) *vs.* HMC. **F** *STAT1* expression levels in BM-1 (n=4) and in MN cells (n=24) normalised *vs.* HMC. Data are presented as mean ± SEM; ** = p≤ 0.01. **E G** Confocal z-stack images showing the immunofluorescent staining of STAT1 (red) and pSTAT1 (Y701- green and S727- red) in MN cells *vs.* HMC. Scale bar 50μm. Nuclei were stained with DAPI (blue).

Fig. 2 STAT1 phosphorylation in meningioma cells is not dependent on the JAK/STAT pathway. **A**WB of WHO I meningioma tumor tissue lysates (n=8); the presence of gamma interferon (IFNγ) and macrophage infiltration (CD163) into the tumor were analysed in relation to STAT1 and pSTAT1 levels. Phospho-JAK1 was used to detect activation of the JAK-STAT pathway (*=positive control for pJAK1 antibody. **B**). WB of total and pSTAT1 in BM-1 and HMC cells, grown in different culture condition. HMC: HMC cells media; MN: MN cells media; MN-SF: MN-serum free media; MN-SF+FBS: MN serum free for 24 h + FBS for 24h; MN Cond: meningioma cells-conditioned media**C** WB analysis of STAT1 and pSTAT1 protein levels in HMC and two primary MN cells after IFNγ treatment at the concentration of 50 ng/ml for the indicated amount of time. Phosho-JAK1 and pJAK2 are shown to confirm the activation of the JAK/STAT pathway. **D** Representative confocal images (z-stack) showing localization of pSTAT1-Y701 (green) and pSTAT1-S727 (red) in primary MN cells before and after IFNγ stimulation (50 ng/ml for 1 h). Scale bar 50µm. Nuclei were stain with DAPI (blue). **E** WB analysis of SOCSs and PIASs protein levels in BM-1 and primary MNs compared to HMC.

559 **Fig. 3** STAT1 overexpression increases meningioma cells proliferation. **A** Histogram representing the
560 percentage of statistical reduction in STAT1 and Cyclin D1 protein levels after *STAT1* sh-RNA-mediated
561 silencing using a pool of three shRNA in 3 primary MN cells compared to scramble; a representative
562 WB is shown underneath. Data are presented as mean ± SD; *** = p≤ 0.001. **B** Percentage of reduction
563 in *STAT1* expression associated to *STAT1* sh-RNA-mediated silencing compared to control shown in
564 **A**; Data are presented as mean ± SEM; **=p≤0.01. **C-D** Representative images of the
565 immunofluorescent staining of STAT1 (green) and the proliferation marker Ki67 (red) (**D**) after *STAT1*
566 sh-RNA-mediated silencing compared to scramble. Nuclei are stain with DAPI (blue). **E-F** Histogram
567 presenting the statistical reduction of proliferating cells and total number of cells (**F**) after STAT1-KD
568 compared to control. Data are presented as mean ± SD; *** = p≤ 0.001, ** = p≤ 0.01. **G** Representative
569 WB, showing the reduction in AKT and ERK1/2 phosphorylation following STAT1 silencing. **H** Histogram
570 representing the WB quantification of total and phosphorylated AKT and ERK1/2 following STAT1
571 silencing in 3 primary MN cells, *** = p≤ 0.001, ns= not significant.

572

Fig. 4 STAT1 activating mutations induce phosphorylation of AKT, ERK1/2 and an increased proliferation of U251-MG cells. **A** WB representing total and phosphorylated STAT1 levels in U251-MG compared to HMC and BM-1 cells. **B** WB showing overexpression of STAT1-WT and activating mutants in U251-MG cells and the related activation of pAKT and pERK1/2. **C** *STAT1* expression levels in U251-MG cells normalised *vs. STAT1* expression levels in pCDNA transfected cells. Data are presented as mean ± SEM; *** = p≤ 0.001. **D** Histogram presenting the statistical increased in cell proliferation in U251-MG cells overexpressing the activating STAT1 mutants (STAT1-Y701F, STAT1-S727E, STAT1-Y701F/S727E). Data were normalised for STAT1-pCDNA-transfected cells and presented as FC of growth *vs.* STAT1-WT; *** = p≤ 0.001.

Fig. 5 The constitutive activation of the EGFR in meningioma induces STAT1 phosphorylation. **A** Representative WB analysis of total and pEGFR-Y1068 in meningioma, when compared to control. Upper panel: WHO I, II and III meningioma tissues compared to NMT; lower panel: BM-1 and primary MN cells compared to HMC. **B** WB of STAT1 and pSTAT1 protein levels after treatment with 5 μM of canertinib, afatinib and erlotinib in BM-1 cells. The reduced levels pEGFR-Y1068 confirmed drug activity. **C** ATP-proliferation assay performed in BM-1 cells after treatment with different concentrations of canertininb, afatinib and erlotinib for 24 h. **D** WB analysis of STAT1, pSTAT1 and other markers of proliferation in primary MN cells after treatment with 10 μM of canertininb. **E H**istograms representing WB quantification at 3 and 24 h for STAT1, pSTAT1, pAKT, pERK 1/2 and Cyclin D1 after canertininb treatment in three different primary MN cells (see Supplementary Fig. 4). Data are presented as mean ± SEM, *= p< 0.05; **= p< 0.01; ***= p< 0.001. **F** q-PCR analysis showing the statistical reduction of *STAT1* gene expression at 3, 6 and 24 h after treatment with 10 μM of canertininb (n=3). Data are presented as mean ± SEM; **= p< 0.01. **G** WB representing STAT1 and pSTAT1 in BM-1 cells, following treatment with EGF (50 ng/ml) for 5, 30 and 60 minutes.

Table

Click here to access/download;Table;Supplementary Table1_NOAR2.docx

Supplementary Table 21. Clinical cases examined in the study. The table provide information about all the meningiomas tested and the level of STAT1 overexpression (gene expression for qPCR and protein expression for WB) detected *vs.* control.-, HMC=Human Meningeal Cells, L=left; R=right; n/a= not available; M=male; F=female, WB= Western Blot; qPCR= quantitative Polymerase Chain Reaction; IF= immunofluorescence; IHC= immunohistochemistry; Control (STAT1 expression = 1); ~ = STAT1 expression below 2; + = 2/3 times STAT1 overexpression; ++ = 5/6 times STAT1 overexpression; +++ = ≥ 10 times STAT1 overexpression.

ID	Type, Location	WHO	Gender	Age of diagnosis	Analysis	STAT1
Ben Men-1 cells	Benign meningioma cell line	I	F	68	WB, qPCR, IF	+
BTNW71 tissue	Anaplastic, L posterior fossa	III	F	70	qPCR	++
BTNW162 tissue	Anaplastic, L fronatl	III	F	76	qPCR	++
BTNW811 tissue	Anaplastic, L posterior fossa	III	F	64	qPCR	++
BTNW831 tissue	Anaplastic ,frontal	III	F	68	qPCR	++
BTNW1456 tissue	Anaplastic, L frontal	III	M	48	qPCR	+
MN001 tissue	Atypical, R frontal	II	M	50	IHC, qPCR	+
MN005 cells	Fibroblastic, L posterior fossa	I	F	59	IHC, qPCR	++
MN015 cells	Psammomatous, cervical	I	F	61	WB, qPCR	+
MN017 cells	Transitional, frontal convexity	I	F	51	WB, qPCR, IF	+
MN020 tissue	Atypical, R parietal	II	F	39	qPCR	~
MN023 cells	Meningothelial, L parietal convexity	I	M	63	WB, qPCR	+++
MN028 cells	Transitional, cervical	I	F	63	WB, qPCR, IF	++
MN031 cells	Psammomatous, thoracic	I	F	72	WB, qPCR, IF	++
MN033 cells	Transitional, -anterior skull base	I	F	65	WB, qPCR, IF	+
MN036 cells	n/a, R CPA	I	F	51	WB, qPCR	++
MN038 cells	Transitional, L parietal	I	F	79	qPCR	+++
MN045 tissue	Atypical, extra axial parietal	II	M	n/a	qPCR	~
MN048 cells	Fibroblastic, L parietal	I	F	57	WB, qPCR	+++
MN052 cells	Psammomatous, R frontal	I	F	70	qPCR	++
MN054 tissue	n/a, R posterior sinus	I	F	58	qPCR	~
MN055 tissue	n/a, L frontal	I	F	50	qPCR	~
MN056 cells	n/a, R posterior fossa	I	F	61	qPCR	++
MN057 cells	Meningothelial, L parietal	I	M	58	qPCR	+++
MN058 tissue	Angiomatous, R~~T~~ frontal	I	F	65	qPCR	~
MN062 cells	Meningothelial, olfactory groove	I	F	43	qPCR	++
MN066 cells	Psammomatous, thoracic~~vertebral~~	I	M	83	qPCR	++
MN071 cells	Secretory/angiomatous, R petroclival	I	F	52	qPCR	++
MN073 cells	Fibroblastic, L convexity	I	F	70	qPCR	++
MN074 cells	Transitional, R angular gyrus	I	F	37	qPCR	+
MN075 tissue/cells	Transitional, R~~T~~ parietal	I	F	79	qPCR	~
MN076 tissue/cells	Atypical, olfactory groove	II	F	53	WB, qPCR	+++
MN077 cells	Transitional, bilateral parasagittal	I	F	66	qPCR	+++
MN078 cells	Transitional, L frontal	I	M	70	qPCR	+++
MN079 tissue/cells	Atypical, occipital	II	M	75	qPCR	~
MN080 cells	Fibrous, L petrous	I	F	64	WB, qPCR	+++
MN082 cells	Fibroblastic, R tentorial	I	F	57	qPCR	+++
MN085 cells	Psammomatous/- fibrous, L frontal	I	F	56	qPCR	+++
MN087 tissue	n/a, CPA	I	M	47	qPCR	~
MN088 tissue	Transitional, sphenoid wing	I	F	n/a	qPCR	~
MN089 cells	Transitional, L parasagittal	I	M	53	qPCR	+++
MN091 cells	n/a, L sphenoid wing	I	F	62	qPCR	+++
MN092 cells	Microcystic, R convexity	I	F	59	qPCR	+++
MN097 tissue	Atypical, L parasagittal recurrent	II	F	66	WB, qPCR	+++
MN101 tissue	Atypical, R~~T~~ frontal	II	F	51	qPCR	++
MN102 cells	n/a, L frontal convexity	I	F	56	qPCR	+++
MN104 tissue	Atypical, R~~T~~ paracentral	II	F	37	qPCR	~
MN105 tissue	Atypical, R~~T~~ frontal	II	F	n/a	qPCR	~
MN106 cells	Psammomatous, planum sphenoid	I	F	46	qPCR	+
MN107 cells	Transitional , R sphenoid wing	I	M	77	qPCR	+++
MN109 cells	Transitional, L posterior frontal	I	F	48	qPCR	+++
MN110 cells	Transitional, L lateral ventricle	I	F	47	qPCR	++
MN113 cells	Secretory, R temporal	I	F	52	qPCR	+++
MN114 cells	Meningothelial, L parasagittal	I	M	62	qPCR	+++
MN115 tissue	Large cystic falcine	I	M	69	qPCR	+
MN125 tissue	Secretory, L~~eft~~ petroclival	I	F	63	qPCR	+++
MN133 tissue	Meningothelial, R fronto-parietal	I	M	87	WB	++
MN139 tissue	Transitional, R sphenoid wing	I	n/a	n/a	qPCR	+
MN140 tissue	n/a, Transitional	I	M	74	qPCR	++
MN148 tissue	Atypical, R~~T~~ frontal	II	M	79	qPCR	~
MN149 tissue	Meningothelial, R frontal	I	n/a	n/a	qPCR	~

Formatted: Indent: Left: 0.1"

Formatted Table

Formatted: Indent: Left: 0.24"

Formatted: Not Highlight

Formatted: Not Highlight

Formatted: Not Highlight

Formatted: Not Highlight

Formatted: Not Highlight

Formatted: Right: -0.29"

ID	Type, Location	WHO	Gender	Age of diagnosis	Analysis	STAT1
MN157 tissue	Meningothelial,extrafrontal	I	F	n/a	qPCR	~
MN168 tissue	Atypica, RT frontal occipital	II	n/a	n/a	qPCR	+
MN170 tissue	Meningothelial, frontal parafalcine	I	F	70	WB, qPCR	+
MN176 tissue	Microcystic, L frontal convexity	I	F	43	WB	~
MN180 tissue	Transitional, R occipital lobe	I	F	45	WB, qPCR	++
MN182 tissue	Atypical, RT fronto-parietal	II	F	66	qPCR	~
MN183 tissue	Chordoid, sellar region	II	F	75	qPCR	~
MN186 tissue	Anaplastic, R temporal	III	M	62	qPCR	~
MN188 tissue	Fibrous, poster fossa	I	F	33	qPCR	~
MN189 tissue	Atypical, left lateral ventricle	II	M	55	qPCR	++
MN194 tissue	Atypical, occipital	II	F	41	qPCR	~
MN196 tissue	Atypical, L parafalcine	II	M	39	qPCR	~
MN200 tissue	Atypical, L fronto-parietal	II	n/a	66	qPCR	+++
MN2078 tissue	Psammomatous, thoracic	I	F	n/a	qPCR	~
MN214 tissue	Meningothelial, olfactory groove	I	F	n/a	qPCR	~
MN217 tissue	Fibrous, R tentorial	I	n/a	n/a	qPCR	++
MN219 tissue	Atypical, L fronto-parafalcine	II	M	55	qPCR	~
MN225 tissue	Atypical, L fronto-parafalcine	II	M	57	qPCR	~
MN234 tissue	Atypical, R fronto-parietal	II	F	79	qPCR	+
MN235 tissue	Atypical, R fronto-parafalcine	II	F	71	qPCR	~
MN242 tissue	Fibrous, olfactory groove	I	F	n/a	qPCR	~
MN248 tissue	MixedTransitional, frontal	I	M	n/a	qPCR	+
MN251 tissue	Fibrous, tentorial	I	F	n/a	qPCR	~
MN252 tissue	Atypical, R parasagittal	II	F	73	qPCR	~
MN261 tissue	Transitional, L parasagittal	I	M	n/a	qPCR	+
MN263 tissue	Atypical, L frontal convexity	II	M	78	qPCR	~
MN274 tissue	Fibrous, L parietal	I	F	68	qPCR	+++
MN278 tissue	Meningothelial, R sphenoid	I	F	n/a	qPCR	+
MN332 tissue	L frontal parafalcine	II	M	68	qPCR	~
MN338 tissue	L temporal convexity	II	F	88	qPCR	++
NH09 tissue	MalignantAnaplastic, occipital	III	n/a	n/a	qPCR	+++
NH10 tissue	MalignantAnaplastic, frontal	III	n/a	n/a	qPCR	+++
J1 tissue	Atypical, sphenoid wing	II	F	62	IHC	++
J2 tissue	Atypical, parafalcine	II	F	51	WB, IHC	++
J3 tissue	Atypical, frontal	II	M	64	WB, IHC	++
J4 tissue	Atypical brain invasion, occipital	II	M	66	WB, IHC, qPCR	+++
J5 tissue	Fibroblastic, occipital	I	F	50	WB, IHC	+++
J6 tissue	Transitional, parasagittal	I	F	37	WB, IHC	+++
J7 tissue	Transitional, parasagittal	I	F	72	WB, IHC	+++
J8 tissue	Transitional, parasagittal	I	F	68	WB, IHC	++
J9 tissue	Malignant, occipital	III	F	82	WB, IHC	++
J10 tissue	Malignant occipital	III	M	85	WB, IHC, qPCR	++
J11 tissue	Malignant, occipital	III	M	85	WB, IHC, qPCR	+++
J12 tissue	Malignant, parasagittal	III	M	87	WB, IHC	++
J22 tissue	Atypical, occipital	II	M	69	qPCR	++
J23 tissue	Atypical, temporal	II	F	62	qPCR	++
nD1 tissue/a	Meningothelial	I	n/a	n/a	IHC	+
n/aD2 tissue	Meningothelial	I	n/a	n/a	IHC	+
n/aD3 tissue	Meningothelial	I	n/a	n/a	IHC	+
n/aD4 tissue	Secretory	I	n/a	n/a	IHC	+++
n/aD5 tissue	Secretory	I	n/a	n/a	IHC	+++
n/aD6 tissue	Secretory	I	n/a	n/a	IHC	++
n/aD7 tissue	Secretory	I	n/a	n/a	IHC	+++
D8 tissuen/a	Secretory	I	n/a	n/a	IHC	+++
D9 tissuen/a	Secretory	I	n/a	n/a	IHC	+
D10 tissuen/a	Transitional	I	n/a	n/a	IHC	++
D11 tissuen/a	Mosaic Fibroblastic	I	n/a	n/a	IHC	+
D12 tissuen/a	Fibroblastic	I	n/a	n/a	IHC	++
D13 tissuen/a	Fibroblastic	I	n/a	n/a	IHC	++
D14 tissuen/a	Psammomatous, spinal	I	n/a	n/a	IHC	++
D15 tissuen/a	Atypical	II	n/a	n/a	IHC	++
D16 tissuen/a	Atypical	II	n/a	n/a	IHC	++
D17 tissuen/a	Atypical, brain invasion	II	n/a	n/a	IHC	++
D18 tissuen/a	Atypical, brain invasion	II	n/a	n/a	IHC	++
D19 tissuen/a	Atypical, brain invasion	II	n/a	n/a	IHC	++
D20 tissuen/a	Malignant	III	n/a	n/a	IHC	++
D21 tissuen/a	Malignant	III	n/a	n/a	IHC	+
D22 tissuen/a	Malignant	III	n/a	n/a	IHC	+

Formatted: Indent: Left: 0.1"

Formatted Table

Formatted: Indent: Left: 0.24"

Formatted: Not Highlight

Formatted: Not Highlight

ID	Type, Location	WHO	Gender	Age of diagnosis	Analysis	STAT1
D23 tissuen/a	Malignant	III	n/a	n/a	IHC	+++
D24 tissuen/a	Malignant	III	n/a	n/a	IHC	++
D25 tissuen/a	Malignant	III	n/a	n/a	IHC	+++
HMC	Human meningeal cells	n/a	n/a	n/a	WB, qPCR, IF	Control
BioChain[R1234043-10]	Cerebral meninges	n/a	F	82	WB, qPCR	Control
ABS[150102416]	Cerebral meninges	n/a	F	92	WB, qPCR	Control
ABS[60200003215]	Cerebral meninges	n/a	F	78	WB, qPCR	Control
n/aC1	Cerebral meninges	n/a	n/a	n/a	IHC	Control
n/aC2	Cerebral meninges	n/a	n/a	n/a	IHC	Control
n/aC3	Cerebral meninges	n/a	n/a	n/a	IHC	Control
n/C4a	Cerebral meninges- glioma	n/a	n/a	n/a	IHC	Control
n/C5a	Cerebral meninges- glioma	n/a	n/a	n/a	IHC	Control
n/C6a	Cerebral meninges- glioma	n/a	n/a	n/a	IHC	Control
Abcam[ab29466]	Brain (human) tissue lysate	n/a	n/a	n/a	WB	+
n/C7a	Normal brain temporal lobe	n/a	n/a	n/a	IHC	Control
n/C8a	Normal brain temporal lobe	n/a	n/a	n/a	IHC	+
n/C9a	Normal brain occipital lobe	n/a	n/a	n/a	IHC	Control
n/C10a	Normal brain frontal lobe	n/a	n/a	n/a	IHC	Control

Formatted: Indent: Left: 0.1"

Formatted Table

Formatted: Indent: Left: 0.24"

Supplementary Table ~~1~~2. Complete list of the antibodies employed in the study, their application and the concentrations used. WB: Western Blot; IF: Immunofluorescence; IP: Immunoprecipitation; IHC: Immunohistochemistry.

Antibody	Manufacturer	Application	Dilution
STAT1	Cell Signaling Technology - #9172	WB	1:1000
	Santa Cruz Biotechnology - sc-592	WB	1:1000
		IF	1:300
		IHC	1:150
pSTAT1-Y701	Abcam - ab29045	WB	1:500
		IF	1:100
	R&D Systems - AF2894	WB	1:1000
		IHC	1:200
	Cell signalling - #7649	WB	1:500
		IP	1:50
pSTAT1-S727	Cell Signaling Technology - #9177	WB	1:1000
		IF	1:100
		IHC	1:400
JAK1	Cell Signaling Technology - #3344	WB	1:1000
pJAK1- Y1022/1023	Cell Signaling Technology - #3331	WB	1:500
JAK2	Cell Signaling Technology - #3230	WB	1:1000
pJAK2- Y1007/1008	Cell Signaling Technology - #3771	WB	1:500
TYK2	Cell Signaling Technology - #14193	WB	1:500
pTYK2- Y1054/1055	Cell Signaling Technology - #9321	WB	1:500
IFN γ	Abcam - ab25101	WB	1:500
CD163	Bio-Rad - MCA1853	WB	1:500
Merlin	Cell Signaling Technology - #6995	WB	1:1000
pMerlin- S518	Cell Signaling Technology - #9163	WB	1:500
ERK	Cell Signaling Technology - #4695	WB	1:2000
pERK- T202/204	BD Biosciences - #612358	WB	1:500
AKT1	Cell Signaling Technology - #4691	WB	1:1000
pAKT1- S473	Cell Signaling Technology - #9271	WB	1:500
RB	Cell Signaling Technology - #9309	WB	1:2000
pRB- S780	Cell Signaling Technology - #8180	WB	1:1000
CD63 (MEM-259)	Thermo Fisher Scientific - MA119281	IF	1:250
CD63	Cambridge Bioscience - EXOAB-CD63A-1	WB	1:500
CD9 (C-4)	Santa Cruz Biotechnology - #13118	IF	1:250
CD9	Cell Signaling Technology - #13174	WB	1:500
GM130	BD Transduction Laboratories - #610823	WB	1:1000
Calnexin (H-70)	SantaCruz Biotechnology - #11397	WB	1:1000
CyclinD1	Cell Signaling Technology - #2978	WB	1: 300
Ki67 (MIB-1)	DAKO - #M7240	IF	1: 1000
PIAS1	Cell Signaling Technology - #3550	WB	1:1000
PIAS3	Cell Signaling Technology - #9042	WB	1:1000
PIAS4	Cell Signaling Technology - #4392	WB	1:1000
SOCS1	Cell Signaling Technology - #3950	WB	1:1000
SOCS2	Cell Signaling Technology - #2779	WB	1:1000
SOCS3	Cell Signaling Technology - #2932	WB	1:1000
EGFR	Cell Signaling Technology - #4267	WB	1:1000
pEGFR- Y1068	Cell Signaling Technology - #3777	WB	1:500
pP70 S6K – T421/S424	Cell Signaling Technology - #9204	WB	1:500
P70 S6K	Cell Signaling Technology - #9202	WB	1:500
GAPDH	EMD Millipore – MAB374	WB	1:50000

Figure

Figure 1

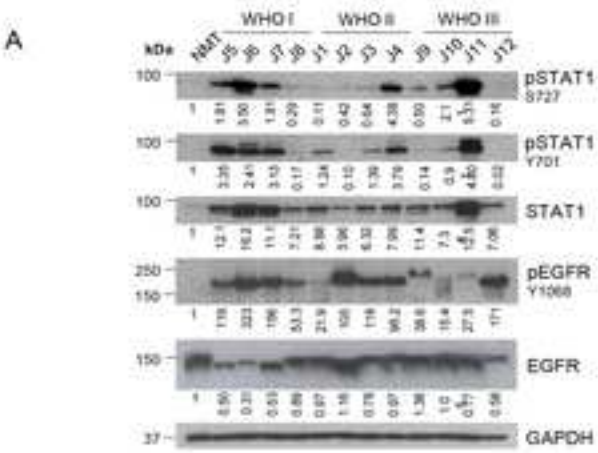

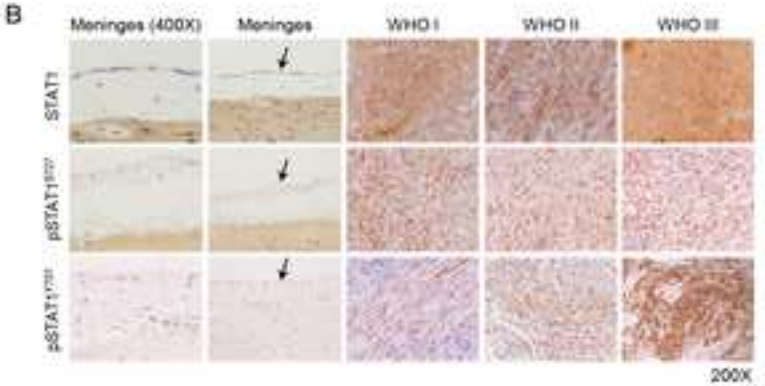

Mean scores (0-3)

Specimen	STAT1	pSTAT1^{Y701}	pSTAT1^{S727}
WHO I (n=19)	2.0	1.0	1.7
WHO II (n=10)	1.7	1.3	1.7
WHO III (n=10)	2.0	2.2	1.9
Normal meninges (n=6)	0	0.16	0.5
Normal brain (n=4)	0.25	0	0.5

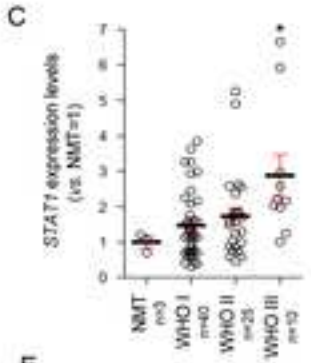

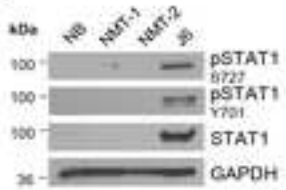

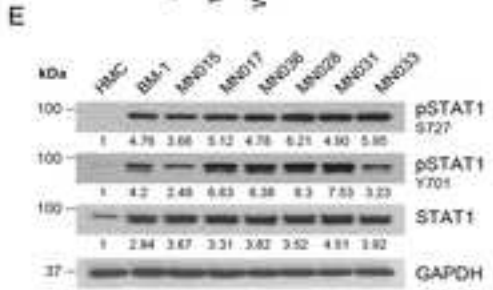

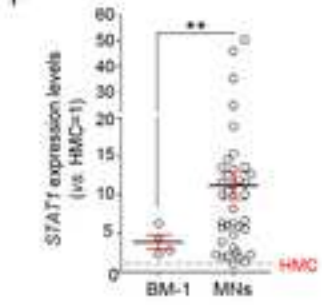

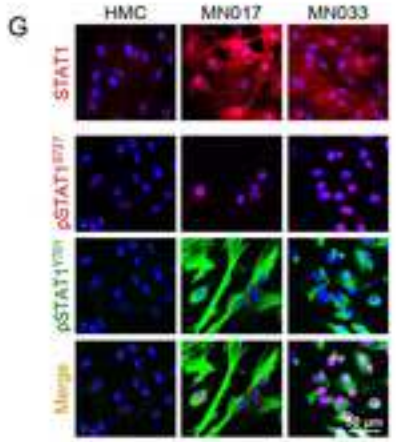

Figure

Figure 2

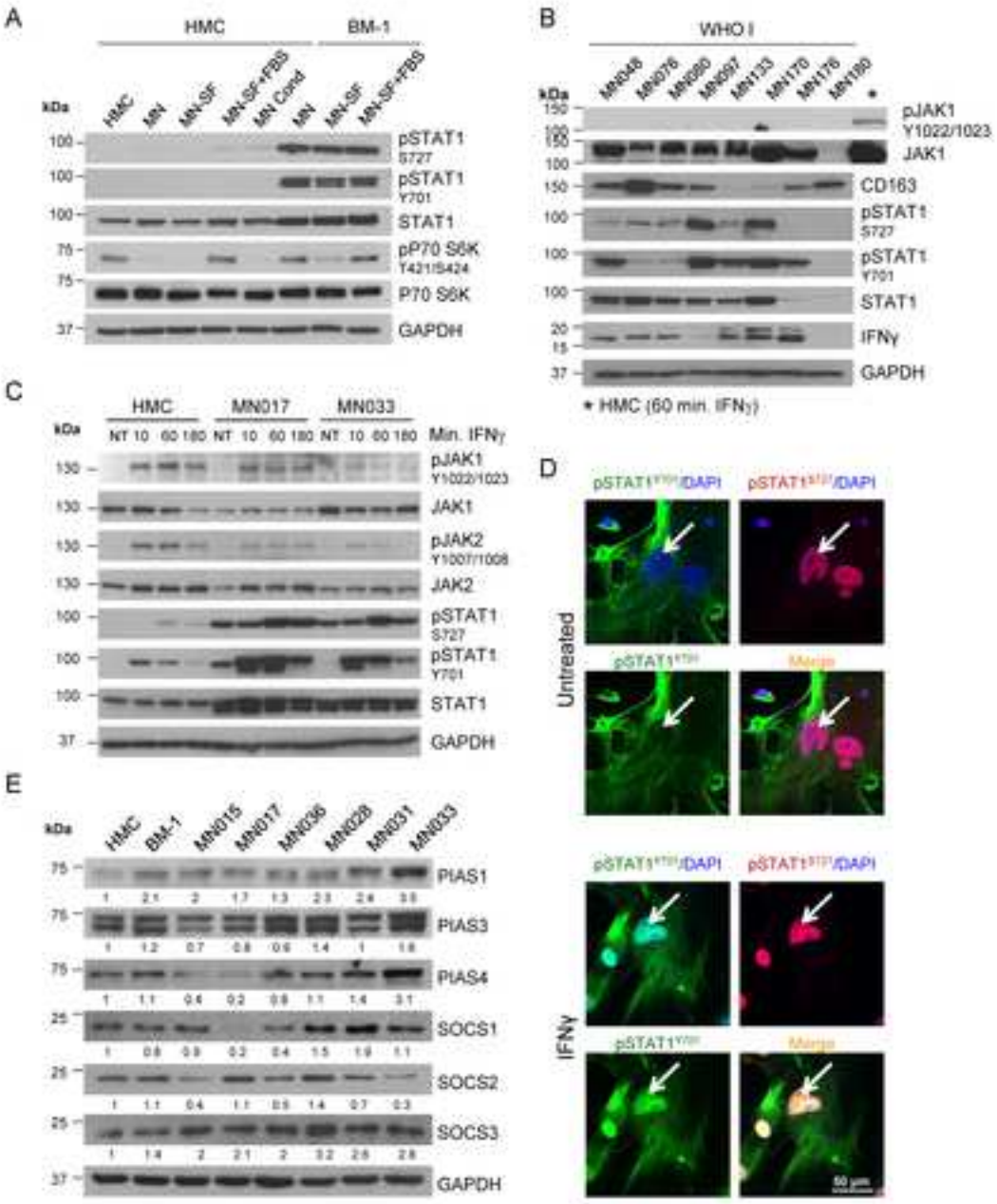

Figure

Figure 3

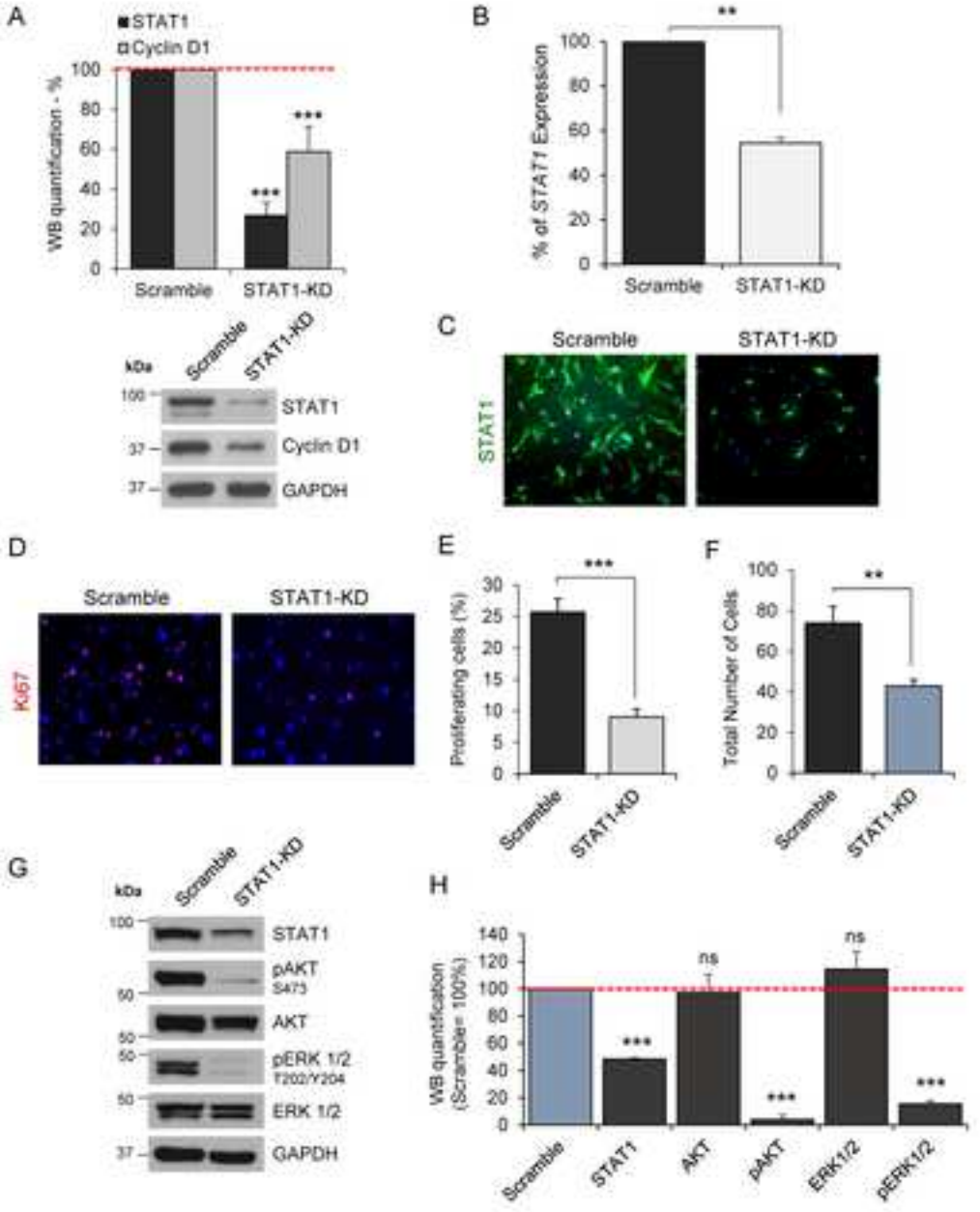

Figure 4

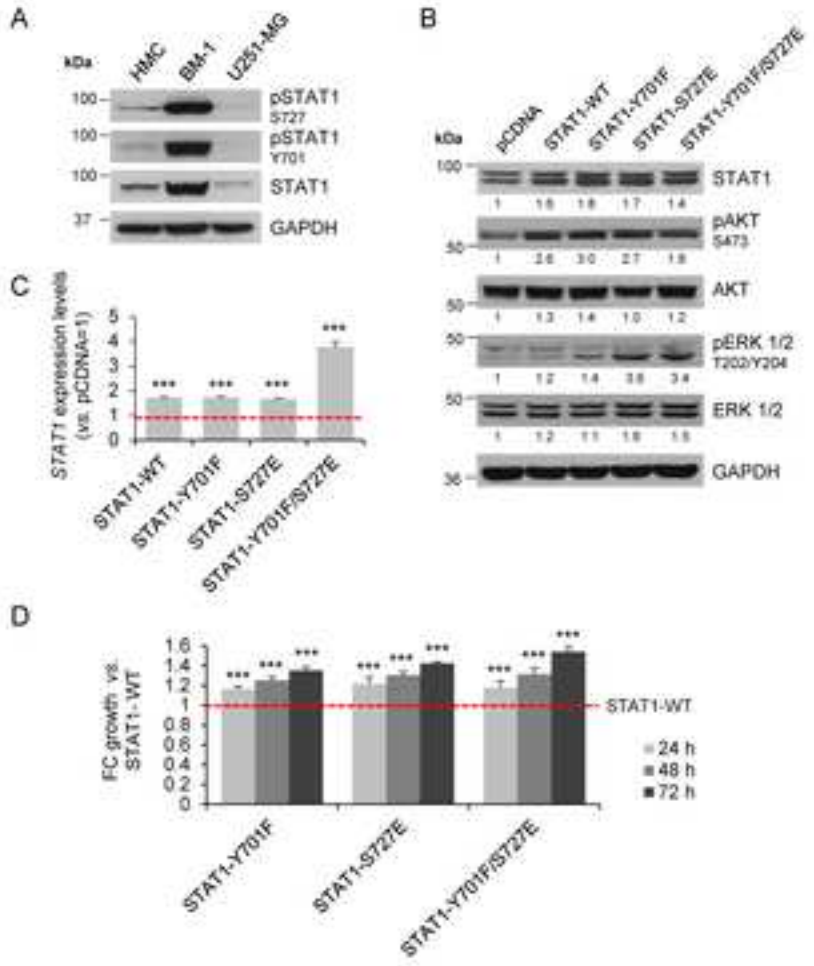

Figure

Click here to access/download;Figure;Figure 5 NOA_revised.tiff

Figure 5

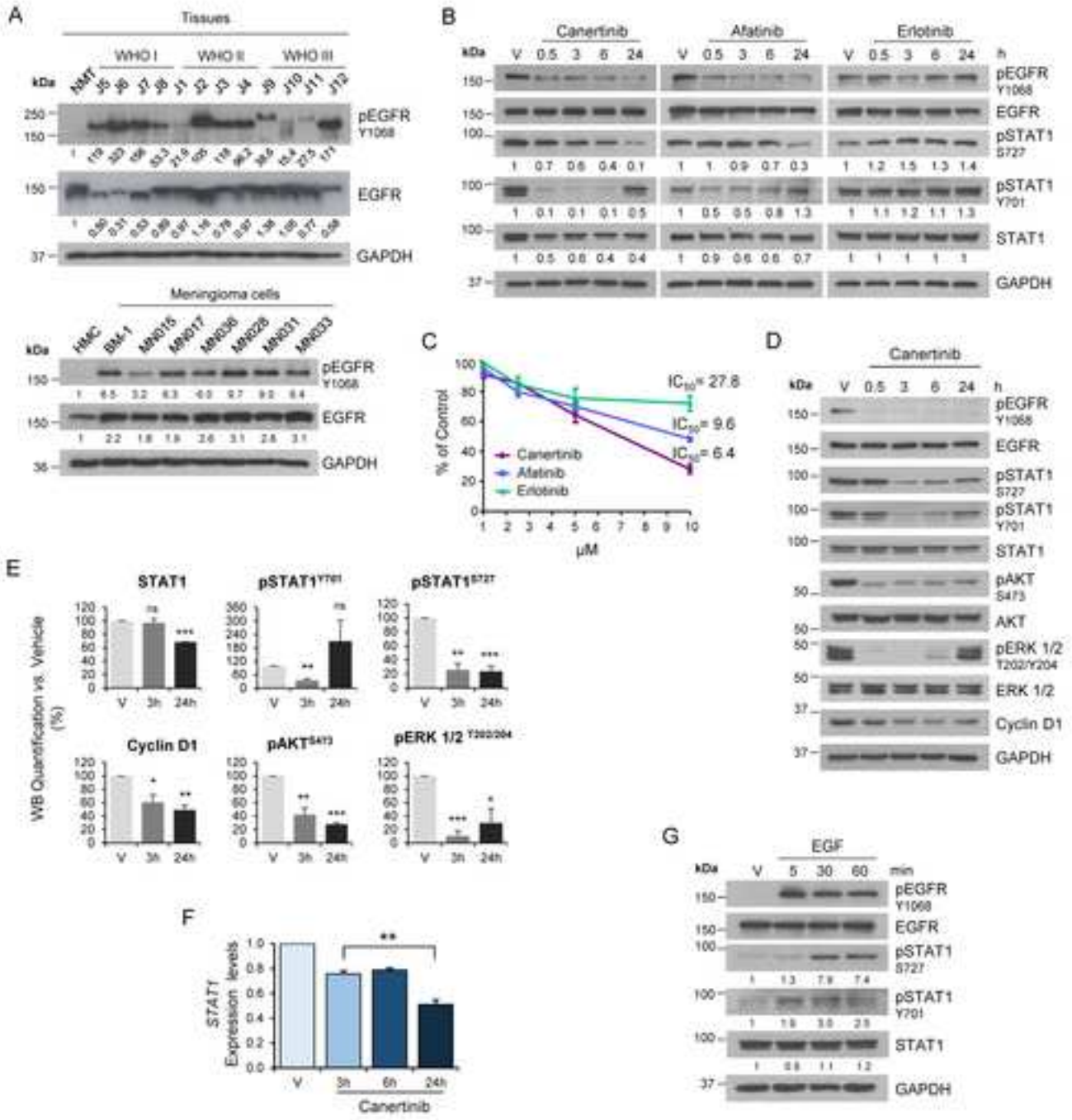

Supplementary File

Supplementary Fig. 1

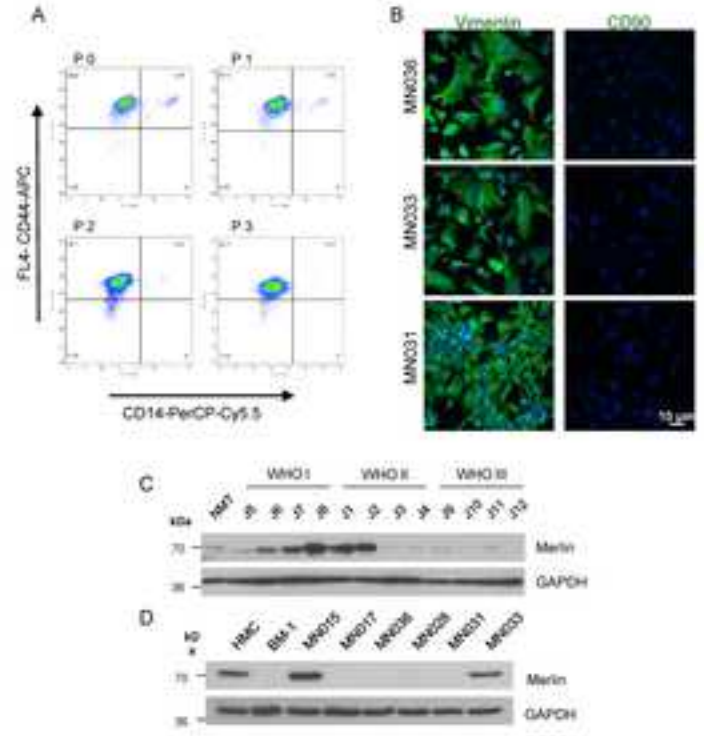

Supplementary File

Supplementary Fig. 2

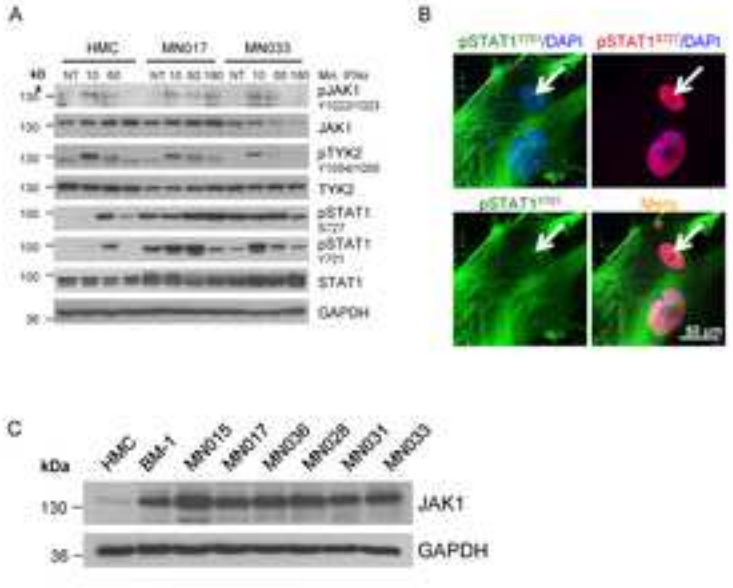

Supplementary Fig. 3

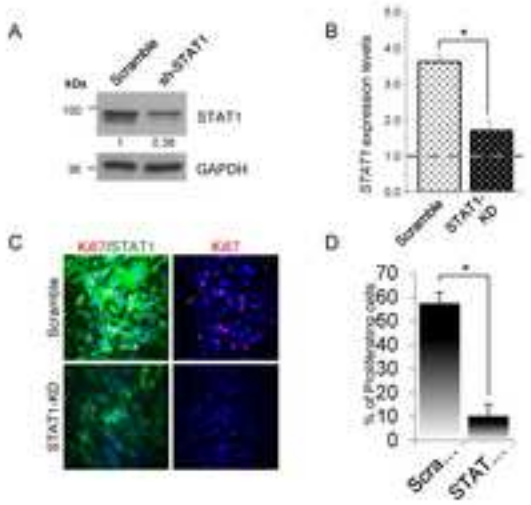

Supplementary Fig. 4

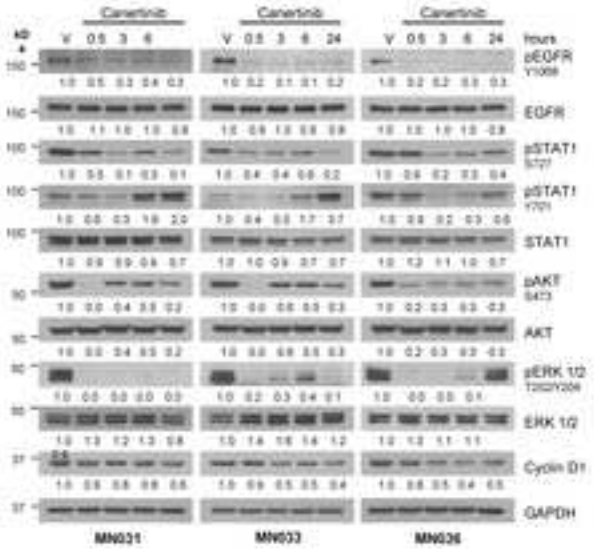

Supplementary Figure Legends

Supplementary Fig. 1 Purity of primary meningioma cultures and genetic background of our cohort of samples. **A** Representative flow cytometry analysis of primary MN cells. Dot plots show 10,000 live cells and represent monocyte marker, CD14-PerCP-Cy5.5 (FL3 channel) and potential meningioma tumour marker, CD44-APC (FL4 channel). Upper right quadrant represents CD14+ CD44+ phenotype and decreases with passage number (CD14+ CD44+ % = Passage 0-4.6, Passage 1-2.1, Passage 2-0.1, Passage 3-0.2). Data analysed was performed on Flow Jo version10.0. **B** Representative confocal images of three primary MN cells tested at passage 3, homogeneously positive for the meningioma marker vimentin (green), while negative for the fibroblast marker CD90. Scale bar 10 μm. Nuclei were stain with DAPI (blue). **C** WB analysis showing the expression of Merlin in different grade meningiomas *vs.* NMT; Next Generation Sequencing (NGS) confirmed that only samples J8, J1 and J2 were Merlin-positive not having any mutation on *Merlin* or loss of heterozygosity (LOH). **D** WB showing the expression of Merlin in in BM-1 and tumour-derived MN cells *vs.* HMC.

Supplementary Fig. 2 The JAK/STAT pathway in meningioma cells can be activated by IFNα. **A** WB analysis of STAT1 and pSTAT1 (Y701 and S727) protein levels in HMC and two primary MN cells, after IFNα treatment at the concentration of 50 ng/ml for the indicated amount of time. Phosho-JAK1 and pTYK2 are shown to confirm the activation of the JAK/STAT pathway. **B** Representative confocal z-stack images showing localization of pSTAT1-Y701 (green) and pSTAT1-S727 (red) in primary MN cells before and after IFNα stimulation (50 ng/ml for 1 h). Scale bar 50 µm. Nuclei were stain with DAPI (blue). **C** Representative WB conducted in primary MN cells showing higher levels of JAK1, when compared to HMC.

Supplementary Fig. 3 STAT1 knocked-down reduces proliferation of BM-1 meningioma cells. **A** WB analysis showing the reduction in STAT1 protein levels after *STAT1* sh-RNA-mediated silencing compared to scramble control. **B** Reduction in *STAT1* gene expression associated to *STAT1* sh-RNA-mediated silencing compared to scramble control. Data are presented as mean ± SEM; * = p≤ 0.05. **C** Representative images of the immunofluorescent staining of STAT1 (green) and the proliferation marker Ki67 (red) after *STAT1* sh-RNA-mediated silencing compared to scramble control. Nuclei are stain with DAPI (blue). **D** Histogram presenting the statistical reduction of proliferating cells after STAT1-KD compared to scramble control. Data are presented as mean ± SD; * = p≤ 0.05.

Supplementary Fig. 4 WB quantification after canertinib treatment in primary MN cells. Detailed WB quantification for the histograms presented in Fig 5E. Protein expression was quantified after normalising for the corresponding GAPDH amount and is presented as fold change of the vehicle-treated sample (V).